Journal of Zhejiang University-SCIENCE B (Biomedicine & Biotechnology) in press
www.jzus.zju.edu.cn; www.springer.com/journal/11585
E-mail: lbwg@zju.edu.cn

Research Article

https://doi.org/10.1631/jzus.B2500083

Hypoxia promotes ovarian cancer progression via Lnc-DARS-AS1/miR-378a-5p/SLC2A12 axis

Wenjie ZENG[1,2,3,4], Hubin XU[5], Huafeng SHOU[2,3,4], Haimin JIANG[5], Mengyu ZHANG[5], Xiaoyan CHEN[2], Weiguo LU[1,6,7] ✉

[1]*Women's Reproductive Health Laboratory of Zhejiang Province, Women's Hospital, Zhejiang University School of Medicine, Hangzhou 310006, China*
[2]*Center for Reproductive Medicine, Department of Gynecology, Zhejiang Provincial People's Hospital (Affiliated People's Hospital), Hangzhou Medical College, Hangzhou 310014, China*
[3]*Key Laboratory of Endocrine Gland Diseases of Zhejiang Province, Hangzhou 310014, China*
[4]*Clinical Research Center for Cancer of Zhejiang Province, Hangzhou 310014, China*
[5]*The Second School of Clinical Medicine, Hangzhou Normal University, Hangzhou 311121, China*
[6]*Zhejiang Key Laboratory of Maternal and Infant Health, Hangzhou 310006, China*
[7]*Zhejiang Provincial Clinical Research Center for Gynecological Diseases, Hangzhou 310006, China*

Abstract: To examine hypoxia-induced alterations in ovarian cancer and elucidate the underlying molecular mechanisms mediated by long non-coding RNAs (lncRNAs). Transwell and MTT assays were performed to assess the migration, invasion and proliferative abilities of ovarian cancer cells. Western blot analysis was conducted to evaluate the expression of factors associated with epithelial-mesenchymal transition (EMT). RNA sequencing was carried out to identify potential targets, and dual-luciferase and biotin-labeled miRNA pull-down assays were performed to identify interactions between these targets. Gain- and loss-of-function experiments were conducted to validate their effects. Hypoxia promoted the migration, invasion, proliferation, and EMT of HO8910 and A2780 cells. Under hypoxic conditions, the expression of Lnc-DARS-AS1 was significantly increased, and this upregulation exerted a proliferative effect on ovarian cancer cells. Furthermore, Lnc-DARS-AS1 promoted solute carrier family 2 member 12 (SLC2A12) expression, accelerating ovarian cancer progression. Luciferase, biotin-labeled miRNA pull-down, and cellular function assays confirmed that Lnc-DARS-AS1 binds to miR-378a-5p to enhance SLC2A12 levels. The expression levels of SLC2A12 were determined in samples from patients with ovarian cancer, and they showed a positive correlation with cancer progression. This research established that the Lnc-DARS-AS1/miR-378a-5p/SLC2A12 axis is involved in ovarian cancer progression under hypoxic conditions, providing new perspectives on the treatment and management of ovarian cancer.

Key words: Hypoxia; Ovarian cancer; Long non-coding RNA DARS-AS1; miR-378a-5p; Solute carrier family 2 member 12; RNA sequencing

1 Introduction

The currently available treatments mainly include debulking surgery, chemotherapy, and the administration of poly(ADP ribose)polymerase (PARP) inhibitor (Chandra et al., 2019).However, chemotherapy resistance poses a critical challenge, as over 70% of patients experience relapse. The key

✉ Weiguo LU, lbwg@zju.edu.cn
Weiguo LU, https://orcid.org/0000-0003-2062-7145
Wenjie ZENG, https://orcid.org/0000-0002-1696-7190

Received Feb. 19, 2025; Revision accepted Nov. 4, 2025;
Crosschecked xxx. xx, 20xx; Published online xxx. xx, 20xx

resistance mechanisms include enhanced DNA repair, evasion of apoptosis, and enhanced drug expulsion through ATP-binding cassette transporters (Colombo et al., 2023). Recent findings indicated that drug resistance is strongly linked to the tumor microenvironment (TME), which promotes tumor survival and reduces chemotherapeutic efficacy through mechanisms such as hypoxia, immune evasion, and metabolic reprogramming (Jiang et al., 2020; Goncalves et al., 2021; Sulaiman et al., 2023). Therefore, it is crucial to understand how the TME affects the development of ovarian cancer.

It is widely acknowledged that hypoxia is a key component of the TME. The rapid growth of tumor cells leads to a hypoxic environment, which in turn promotes tumor growth through the release of multiple growth factors and cytokines, the most common of which is hypoxia-inducible factor 1 (HIF-1). Notably, the growth environment under hypoxic conditions can significantly affect the physiological characteristics and treatment responses of ovarian cancer cells. Several studies have revealed that ovarian cancer cells often exhibit significant changes in growth and metastasis under low oxygen conditions (Zhang et al., 2018). This hypoxic state within tumor tissues causes tumor cells to adapt to the environment by regulating gene expression and signaling pathways, thereby promoting tumor growth and invasion. Despite these findings, the precise molecular mechanisms through which hypoxia influences ovarian cancer progression, particularly the function of long non-coding RNAs (lncRNAs) in this process, remain poorly understood. Therefore, understanding the impact of hypoxia on ovarian cancer can not only help explore its pathogenic mechanisms but also provides important insights for developing more effective treatment strategies.

LncRNAs are a type of non-coding RNAs that exceed 200 nucleotides in length and serve a crucial regulatory function within cells (Peng et al., 2017). In the recent decades, many studies have demonstrated that lncRNAs are critical mediators in various cancers, regulating gene expression, signaling pathways, and cellular functions, as well as in influencing tumor occurrence, development, and treatment response (Mccabe and Rasmussen, 2021; Tan et al., 2021; Hashemi et al., 2022). Research indicates that lncRNAs affect ovarian cancer cell proliferation, apoptosis, invasion, and metastasis, thereby impacting tumor malignancy and prognosis (Braga et al., 2020; Yang et al., 2023). For example, the lncRNA LUCAT1 affects the biological activity of tumor cells in ovarian cancer by regulating miRNA or protein expression, thus affecting ovarian cancer progression (Xing et al., 2021). Nonetheless, the specific function of Lnc-DARS-AS1 in ovarian cancer metastasis under hypoxic conditions has not been fully explored. Currently, a well-recognized finding is that there is a competition between lncRNAs and protein-coding mRNAs for miRNA binding, known as competitive endogenous RNA (ceRNA) activity. Salmena et al. (Salmena et al., 2011) hypothesized that miRNA response elements form a complex interaction network involving miRNAs, lncRNA transcripts, protein-coding genes, and pseudogenes. In addition, direct interactions between lncRNAs and proteins or mRNAs have been observed, such as those between the lncRNA FAM225B and the mRNA of the DDX17 gene (Liu et al., 2020). Furthermore, lncRNAs have demonstrated clinical value as both therapeutic targets and indicators for diagnosis and prognosis in a range of cancers, including ovarian cancer (Abildgaard et al., 2019).

While long non-coding RNAs have been increasingly recognized as key regulators in cancer progression, their specific roles in mediating hypoxia-induced metabolic reprogramming through glucose transporter regulation remain poorly understood. This study newly identifies a hypoxia-responsive axis centered on Lnc-DARS-AS1, which functions as a competing endogenous RNA that sequesters miR-378a-5p to regulate solute carrier family 2 member 12 (SLC2A12) expression. Unlike the well-characterized hypoxia-inducible factor 1-alpha (HIF-1α)-mediated regulation of SLC2A1 (Seeber et al., 2011), the Lnc-DARS-AS1/miR-378a-5p/SLC2A12 axis represents a distinct post-transcriptional mechanism that expands our understanding of metabolic adaptation in ovarian cancer. This study examined hypoxia-induced alterations in ovarian cancer and elucidated the underlying molecular mechanisms mediated by lncRNAs, with the aim of advancing the understanding of ovarian cancer, supporting precision therapy, and ultimately reducing its profound impact on women's health.

2 Materials and methods

2.1 Cell culture

HO8910 and A2780 cells (ATCC, China) were incubated at 37 °C in a 5% (v/v) CO2 incubator using high-glucose DMEM medium (Gibco, USA) supplemented with 10% (v/v) fetal bovine serum (FBS, Gibco) and 1% (v/v) penicillin-streptomycin. For hypoxia experiments, cells were transferred to a tri-gas incubator (Thermo Fisher Scientific, 4131, USA). According to the pre-experimental results, A2780 cells were grown in normal or hypoxic (1% (v/v) oxygen) conditions for 2 h, whereas HO8910 cells were grown in either normal oxygen levels or hypoxic (1% (v/v) oxygen) conditions for 24 h.

2.2 Cell transfection

For overexpression plasmid transfections, 2 μL of Lipofectamine 2000 (Invitrogen, USA) was mixed with 50 μL of Opti-MEM I Reduced Serum Medium (Gibco) and incubated for 5 min. Similarly, 2 μL of miR-378a-5p mimics (Hippobio, Huzhou, China) or 6 μg of SLC2A12 or Lnc-DARS-AS1 plasmids (Guannan Bio, China) were mixed with 50 μL of Opti-MEM I Reduced Serum Medium and incubated for 5 min. The two solutions were then combined and incubated for an additional 20 min.

Small interfering RNAs (siRNAs) targeting SLC2A12 (siR-SLC2A12) and Lnc-DARS-AS1 (siR-Lnc-DARS-AS1) (Hippobio, Huzhou, China) were transfected into HO8910 and A2780 cells at 70-80% confluence in 6-well plates. The transfection complex was prepared by mixing 2 μL of siRNA (100 nmol/L final concentration) with 2 μL of Lipofectamine 2000 in Opti-MEM I Reduced Serum Medium. The respective sequences are provided in Table 1. Cells were then incubated with the mixture for 24 or 48 h before subsequent experiments.

Table 1 siRNAs sequences

Name	Sequence
NC siRNA	sense: UUCUCCGAACGAGUCACGUTT antisense: ACGUGACUCGUUCGGAGAATT
siR-SLC2A12-1	sense: GCCCAUAUAUUCUAUCUAGAU antisense: AUCUAGAUAGAAUAUAUGGGC
siR-SLC2A12-2	sense: CGGCAUUCUUUCUGCCUAUAU antisense: AUAUAGGCAGAAAGAAUGCCG
siR-SLC2A12-3	sense: CCUUGCUAAAUGCUGGAUUAA antisense: UUAAUCCAGCAUUUAGCAAGG
siR-DARS-AS1-1	sense: GGACUAUAUCUUAAGACUAUG antisense: CAUAGUCUUAAGAUAUAGUCC
siR-DARS-AS1-2	sense: GCAUAGAGUCAACGUUGAAGG antisense: CCUUCAACGUUGACUCUAUGC

2.3 Cell proliferation assay

Cells treated as needed (3×104 cells/mL) were cultured for 0, 24, 48, 72, and 96 h in a 96-well plate. The medium was removed, and 50 μL of methylthiazolyldiphenyl-tetrazolium bromide (MTT, M2128, Sigma, USA) solution was added to each well for three hours of incubation. Then, 150 μL of DMSO was added to each well and mixed thoroughly. The optical density at 570 nm was finally measured to assess the proliferation capability of ovarian cancer cells.

2.4 Transwell assay

To evaluate the metastasis of HO8910 and A2780 cells, a Transwell assay was conducted. The Matrigel (356234, Corning, USA) was first mixed with serum-free medium at a 1:40 ratio at 4 °C. For the invasion

experiment, the upper layer of the Transwell chamber (8.0 μm, 3422, Corning, USA) was coated with Matrigel and incubated at 37 °C for half an hour. Then, the cells were seeded in serum-free medium on the upper layer of the culture chamber and incubated for 24 h. The invading cells were fixed with 500 μL of methanol for 20 min and stained with 20 g/L crystal violet (C110703, Aladdin, China) for 40 min. Finally, more than three randomly selected fields were photographed for counting and statistical analysis. For the migration test, the specified cells were placed in the upper section of the chamber without the Matrigel. The remaining steps were identical to those used in the invasion experiment.

2.5 Western blot (WB) assay

Cells were lysed with protein lysis buffer on ice for 10 min, followed by protein quantification using a BCA kit (Sigma). After separation by SDS-PAGE gel, the protein samples were transferred to a PVDF membrane and blocked with 50 g/L bovine serum albumin (BSA) for 2 h. The PVDF membrane was incubated with the primary antibodies (Proteintech) at 4 °C overnight and with the secondary antibodies (Proteintech) at 22 °C for 2 h. Finally, an ECL kit (Bio-Rad, USA) was used to detect the protein bands, which were then quantified using ImageJ software. Details of the antibodies used are listed in Table 2.

Table 2 Details of antibodies used in the study

Name	Brand	Catalog number	Dilution rate	Applications
E-cadherin	CST	3195S	1:1000	WB
N-cadherin	Proteintech	22018-1-AP	1:16000	WB
Vimentin	CST	5741T	1:1000	WB
HIF-1α	Proteintech	20960-1-AP	1:12000/1:500	WB/IHC
MMP9	Proteintech	10375-2-AP	1:3000	WB
MMP2	Proteintech	10373-2-AP	1:1000	WB
SLC2A12	Proteintech	26958-1-AP	1:1000/1:500	WB/IHC
Flag	Proteintech	66008-4-Ig	1:50000	WB
β-actin	Proteintech	20536-1-AP	1:10000	WB

IHC, immunohistochemistry; WB, western blot

2.6 Quantitative real-time PCR

Total RNA was extracted from the cells using TRIzol reagent (Sigma). A NanoDrop reader (Thermo Fisher Scientific, 2000/2000c) was used to measure RNA concentration and assess RNA quality using the OD260/OD280 and OD230/OD260 ratios. A reverse transcription kit (Promega, USA) was employed to transcribe RNA into cDNA, followed by amplification with a 2×SYBR Green qPCR MasterMix (Thermo Fisher Scientific) by a quantitative real-time PCR (qRT-PCR) instrument (Thermo Fisher Scientific 7300). The results were calculated using the $2^{-\Delta\Delta Ct}$ method. The primers used are listed in Table 3.

Table 3 Primer sequence details

Name	Forward (5'-3')	Rear (5'-3')
β-actin	AGCAGTTGTAGCTACCCGCCCA	GGCGGGCACGTTGAAGGTCT

U6	CTCGCTTCGGCAGCACA	AACGCTTCACGAATTTGCGT
GPRC5D-AS1	CCTCCAGAGTTTACTGCCATGAC	GTAGGATCTCCGCCACTGATTC
TP53TG1-AS1	ACACCCGATTCAAAGTGG	GTTGGGAAATGTGAGCAA
TTC28-AS1	AGCGCTCGTAGAGGTACTCA	TCGTGCTTGTGTCATCCAGG
NEAT1	GGCAGGTCTAGTTTGGGCAT	CCTCATCCCTCCCAGTACCA
CYP1B1-AS1	ACACAAGAATCGGCACTGGT	CCAGTACACCCCTCTCAGGT
TMEM147-AS1	CTGAAACAGCCAAGGTGTGC	TCTAGGAGGGTTCATGGCGA
FOXP4-AS1	AGCTTCTGGGTTCGACAGTG	AGGAGTCCGGAATGACCTGA
OGFR-AS1	GAGGTGGGTGCCTTGTGA	TGCGGCTGTGAGATGAGA
DARS-AS1	GGCTTCTCCTGACTCTTG	TCTTCCTGTACTGGTGGG
ITGA6-AS1	AGGTGGCAACATCCCTACAC	AGCTCCAGCCTTGTTTCCAA
OXTR	CTACCTGCTGCTGCTCATGT	ATGACCGGCACGATGTAGAC
THEMIS2	GTGGTCTGTGAGAACCCGAA	CATCACCACAGCCTCAAGCA
TCF7L1	GGACTATTTCGCCGAAGTGA	ATGTGATGCGGGTGCTGA
SLC2A12	GCCCCTGAGAAATGATGTGG	GAGGAGATTGATGCCCCAGTT
ATXN7	TTCCCACTCACACACTCCTCT	CCTGTTCGTAAGCAAGGTGAG
AMPD3	CCCTGTCGTCCGAACCC	GGGACTGGGACCGAATCATC
LETMD1	CCTGGTCTTCTTGCTAATG	AAAGCCTGGAGTTGGTTC
EDEM1	CGGGGACCCTTCAAATCT	TGGGCCATGTATAACAACTC
EDEM2	ACTACAGGGAGCGAGTCAA	TCCTGGAGCACTTCAACC
EDEM3	TTCCAGATGGCAGGTGATGG	CAACCAAATCAACCTCCTGAGA
miR-378a-5p	CGAGGTATTCGCACT	TCCTGACTCCAGGTC
SLC2A12	ACAGTGTCCAATTCTTCACA	GTCCTGATGTCTGAATGTCA

2.7 Dual-luciferase reporter assay

The dual-luciferase reporter assay was conducted to validate the relationship among Lnc-DARS-AS1, miR-378a-5p, and SLC2A12. Wild-type and mutant luciferase reporter plasmids for SLC2A12 and

Lnc-DARS-AS1 were constructed as follows: fragments corresponding to the wild-type 3' UTR of SLC2A12 (nucleotide positions 821–1027, GenBank accession NM_145176) or the wild-type sequence of Lnc-DARS-AS1 (positions 215–420, NR_110199) were inserted into the pmirGLO dual-luciferase vector (Promega) using the EcoRI and BamHI restriction sites. Mutant versions were generated by introducing nucleotide substitutions within the putative miR-378a-5p binding sites, as predicted by the miRDB database for SLC2A12 and by an lncRNA–RNA interaction prediction tool for Lnc-DARS-AS1. All plasmid constructs were commercially synthesized by Youbio Biological (Hunan, China).

For functional validation, HO8910 cells were co-transfected with the respective reporter plasmids along with Lnc-DARS-AS1 overexpression plasmids, miR-378a-5p mimics, and negative controls for 24 h to determine the relationship between SLC2A12, miR-378a-5p, and Lnc-DARS-AS1. Luciferase activity was measured using a dual-luciferase reporter system (Promega). HO8910 cells were lysed and centrifuged at 14,000 r/min for 20 min. The lysates were then analyzed using the Promega GloMax 96 Microplate Chemiluminescence Detector. Then, 50 μL of Stop&Glo® Reagent (Promega) was added for analysis. Relative fluorescence intensity was calculated based on these two values. The detailed sequences are provided in Table 4, with mutation sites indicated in bold.

Table 4 Details of SLC2A12 reporter gene

Construct name	Sequence
SLC2A12 3’UTR-WT	ATTAGGTTGAAGTTATTAAGTCAAGCCTAGAAAAGCTGCCTC CTTGTAAGGCTTTCATGACAATGTATAGTAATCCACAGTGTCCAA TTCTTCACACTCCTCAGGAATATCACTACCTCAGGTTACGGTACA CAGGCTATAATTGATGATGATGTTCAGATAACTGAAGACACAATA AATGACATTCAGACATCAGGACAATTCCCT
SLC2A12 3’UTR-MUT	ATTAGGTTGAAGTTATTAAGTCAAGCCTAGAAAAGCTGCCTC CTTGTAAGGCTTTCATGACAATGTATAGTAATCCACAGTGTCCAA TTCTTCACACTCCAGTCCTTTATCACTACCTCAGGTTACGGTACAC AGGCTATAATTGATGATGATGTTCAGATAACTGAAGACACAATA AATGACATTCAGACATCAGGACAATTCCCT
DARS-AS1 3’UTR-WT	GGAGGAAACCCACTTCCGCCGCGTCCATGATCTCCCGCGGCT TCTCCTGACTCTTGCGGCTGGCGCTGGCGCTGGGCATCGGGACAC GGAACTGGGCAGTGGACACCACCCTCCCTCGCAGGCTTCCAAAGT AATTTGAAGGCCTTCCCTGACTTAAAGTGGATGCTGCTTTGGAAA GCACTGGAAAAATGGATCCTGTCTTTCTT
DARS-AS1 3’UTR-MUT	GGAGGAAACCCACTTCCGCCGCGTCCATGATCTCCCGCGGCT TCTCCTGACTCTTGCGGCTGGCGCTGGCGCTGGGCATCGGGACAC GGAACTGGGCAGTCCTGTGCACCCTCCCTCGCAGGCTTCCAAAGT AATTTGAAGGCCTTCCCTGACTTAAAGTGGATGCTGCTTTGGAAA GCACTGGAAAAATGGATCCTGTCTTTCTT

2.8 Biotin-labeled miRNA pull-down assay

HO8910 cells were transfected with biotin-labeled miR-378a-5p mimics or biotin-labeled negative control RNA (hippoBio) using Lipofectamine 2000. After 24 h, cells were harvested and lysed. To capture the biotin-labeled RNA complexes, the cell lysates were incubated with Dynabeads™ M-270 streptavidin beads (Thermo Fisher Scientific, 65305) at 4 °C for 4 h. Subsequently, the beads were washed extensively with wash buffer to remove non-specifically bound materials. Finally, RNA was extracted from the beads using TRIzol reagent, and the enrichment of Lnc-DARS-AS1 and SLC2A12 was quantified by qRT-qPCR. The results were normalized to input controls and compared to the negative control group to confirm specific binding interactions.

2.9 RNA-sequencing analysis

RNAs were extracted from HO8910 cells cultured under normoxic or hypoxic conditions for 24 h. lncRNA

sequencing was performed by Hangzhou Kaitai Biotechnology Co., Ltd. RNA from Lnc-DARS-AS1 overexpressing HO8910 cells was collected, and mRNA sequencing was conducted by Beijing Novozymes Biotechnology Co., Ltd.

2.10 Bioinformatics analysis

Heatmaps and volcano plots were used to present differentially expressed genes (DEGs), which were enriched in signaling pathways using Gene Ontology (GO) and KEGG enrichment analyses. The binding site between SLC2A12 and Lnc-DARS-AS1 was predicted using StarBase (https://rnasysu.com/encori/index.php). R software was used to examine the relationship between SLC2A12 and ovarian cancer, with patient data sourced from The Cancer Genome Atlas (TCGA) database.

To evaluate the clinical relevance of SLC2A12, 428 ovarian cancer samples from TCGA were divided into high- and low-expression groups based on the median expression level (2.016885). Clinical features including age (≤65 vs. >65 years), race (white vs. non-white), and stage (grouped as Low Burden [Stage I/II/IIIA/IIIB], Stage IIIC, and Stage IV) were compared using the CreateTableOne function from the R package "tableone" (v 0.13.2).

The correlation between SLC2A12 and HIF-1α expression was analyzed using the GSE218939 dataset, which includes 22 primary and 29 metastatic ovarian cancer samples. The expression matrices were extracted and analyzed using the "ggcorrplot" (v 0.1.4.1) and "corrplot" (v 0.94) packages, with scatter plots generated via "ggplot2" (v 3.5.1).

For miRNA analysis, the GSE261800 dataset comprising 20 ovarian cancer and 20 adjacent normal samples was analyzed using "DESeq2" (v 1.48.1) under thresholds of $p<0.05$ and $|\log_2 FC|>1$. Meanwhile, miRNAs targeting SLC2A12 were predicted via the miRDB database. A Venn diagram was subsequently generated using the R package "ggvenn" (v 0.1.16) to visualize the overlap between these DEGs and the ER stress-related gene set.

In ovarian cancer and adjacent tissue samples from the GSE261800 dataset, the expression of hsa-miR-378a-5p was analyzed for intergroup differences using the Wilcoxon rank-sum test from the R package"ggpubr" (v 0.6.1).

2.11 Clinical samples

Paraffin sections from 20 pairs of primary and metastatic foci were obtained from patients with ovarian cancer at Zhejiang Provincial People's Hospital between January and December 2022. Informed consent was obtained from all patients. This study was approved by the Ethics Committee of Zhejiang Provincial People's Hospital and conducted following the guidelines of the Declaration of Helsinki.

2.12 Immunohistochemistry assay

The tissue sections were subjected to microwave antigen retrieval and blocked with 30 g/L BSA, then they were then incubated with SLC2A12 and HIF-1α antibodies overnight. The slices were washed with PBS and subsequently incubated with the secondary antibody for 2 h. Nuclei were stained with hematoxylin for 3 min. After staining, coverslips were mounted on the sections, which were then observed under a microscope and scanned.

2.13 Hematoxylin-eosin staining assay

Sections were sequentially deparaffinized using xylene and graded alcohol concentrations, followed by staining with hematoxylin for 10 min and eosin for 3 min. After staining, the sections were treated with alcohol for dehydration and with xylene for clearing, then mounted with coverslips, observed under a microscope, and scanned.

2.14 Statistical analysis

Each experiment was performed three times, with the results shown as mean ± standard deviation. Data analysis was carried out using SPSS Statistics 25, applying one-way ANOVA or the Kruskal-Wallis H test for multiple group comparisons and Student's t-test for two-group comparisons. Significance was set at $p<0.05$.

3 Results

3.1 Malignant phenotypes of ovarian cancer cells promoted by hypoxia

The migration and invasion abilities of ovarian cancer cells were notably enhanced under hypoxic conditions (Fig. 1a), and the cells showed a marked decrease in proliferative capacity when exposed to hypoxic conditions (Fig. 1b). The protein level of HIF-1α (a hypoxic biomarker) was significantly elevated under hypoxia. To further investigate the effects of hypoxia, we examined epithelial-mesenchymal transition (EMT)-related factors that are closely associated with tumor aggressiveness. Hypoxia increased the EMT potential of ovarian cancer cells, resulting in a higher expression of N-cadherin, matrix metallopeptidase 2 (MMP2), matrix metallopeptidase 9 (MMP9), and vimentin, and a lower expression of E-cadherin (Fig. 1c). These results demonstrated that hypoxia triggered malignant progression in both HO8910 and A2780 cells.

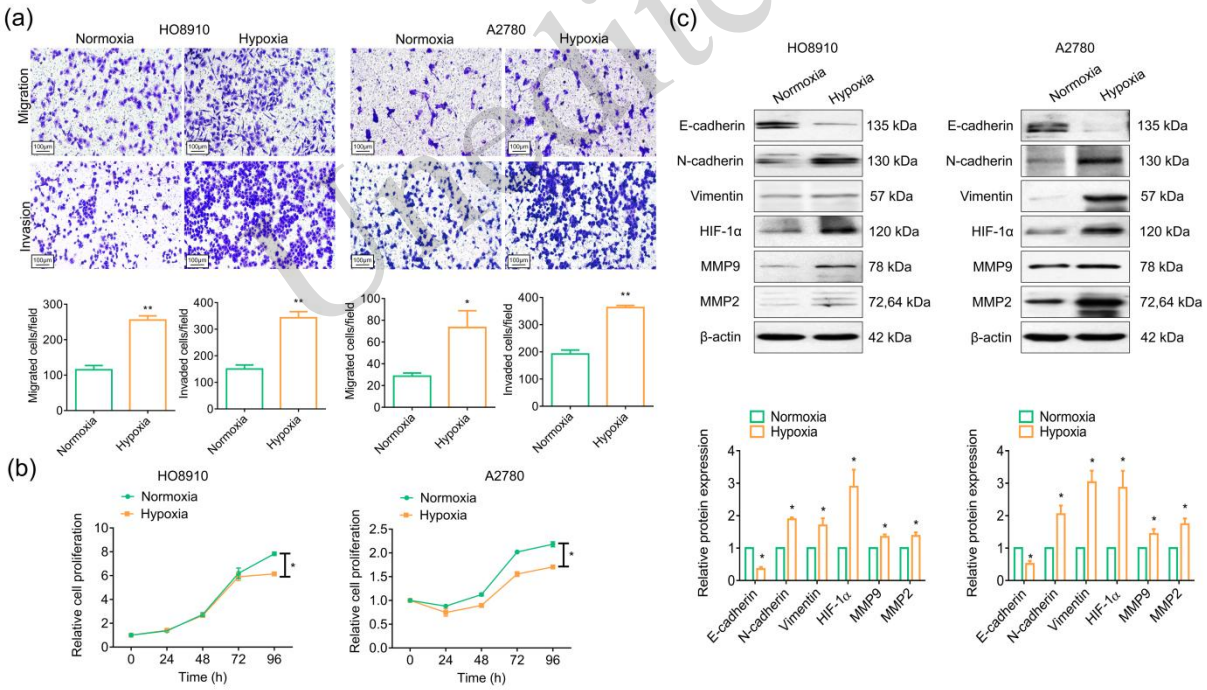

Fig. 1 Effect of hypoxia on the malignant progression of ovarian cancer cell lines. (a) Transwell assays were used to evaluate the migration and invasion abilities of HO8910 and A2780 cells under normoxic or hypoxic conditions for 24 h. (b) MTT assays were used to evaluate the proliferation ability of HO8910 and A2780 cells. (c) The expression levels of HIF-1α and epithelial-mesenchymal transition (EMT)-related factors were detected by western blot assays. All experiments were repeated three times. *$p<0.05$, **$p<0.01$. HIF-1α, hypoxia-inducible factor 1-alpha.

3.2 The malignant phenotypes of ovarian cancer cells enhanced by hypoxia-induced Lnc-DARS-AS1

To explore how hypoxia influences ovarian cancer progression, we performed lncRNA sequencing analysis on HO8910 cells cultured under normoxic and hypoxic conditions (Fig. 2a). A total of 505 lncRNAs were significantly upregulated and 535 lncRNAs were downregulated in HO8910 cells under hypoxic conditions, suggesting that hypoxia may regulate ovarian cancer progression by deregulating lncRNA

expression (Fig. 2b). Furthermore, Lnc-DARS-AS1 was the most significantly upregulated lncRNAs in ovarian cancer cells under hypoxic conditions (Fig. 2c). By constructing Lnc-DARS-AS1 overexpressing HO8910 and A2780 cells, we explored the role of Lnc-DARS-AS1 in ovarian cancer (Fig. 2d). It was observed that Lnc-DARS-AS1 levels were positively associated with the migration and invasion capabilities of HO8910 and A2780 cells (Fig. 2e). Interestingly, ovarian cancer cell proliferation was enhanced by overexpressing Lnc-DARS-AS1 in HO8910 and A2780 cells (Fig. 2f). Moreover, high Lnc-DARS-AS1 expression induced EMT, notably enhancing the levels of N-cadherin and vimentin while reducing the level of E-cadherin (Fig. 2g). These findings indicate that Lnc-DARS-AS1 may serve as an oncogene involved in hypoxia-induced ovarian cancer progression.

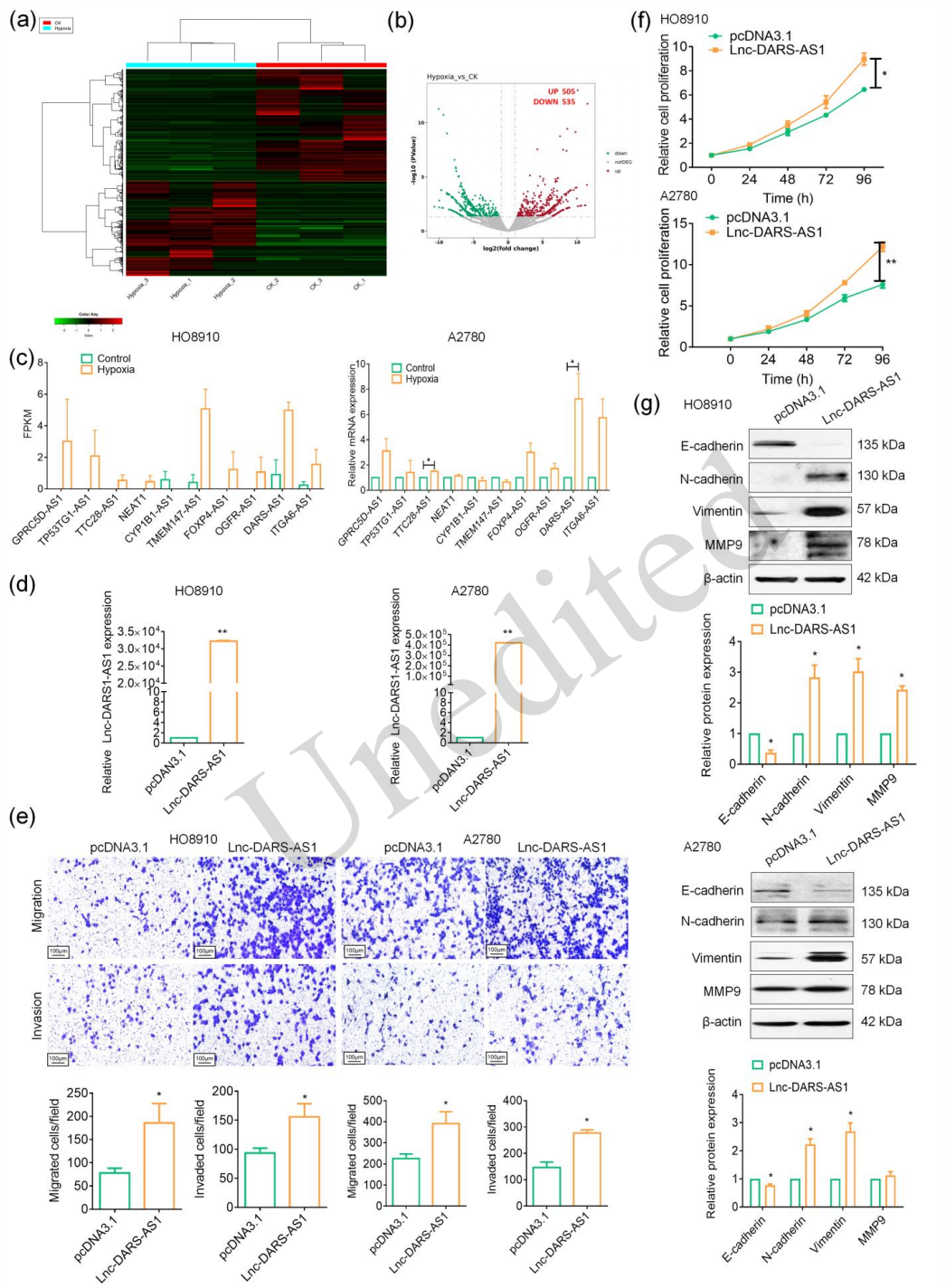

Fig. 2 Effect of Lnc-DARS-AS1 overexpression on the malignant phenotype of ovarian cancer cells. (a-b) LncRNA sequencing analysis was performed on HO8910 cells under normoxic and hypoxic conditions. The results of differentially expressed lncRNAs (DElncRNAs) in HO8910 cells under hypoxia are presented as a heatmap (a) and a volcano plot (b). (c) The top 10 DElncRNAs were examined by quantitative real-time PCR (qRT-PCR) assay in HO8910 and A2780 cells. (d) qRT-PCR was used to evaluate the overexpression efficiency of Lnc-DARS-AS1. (e) The migration and invasion abilities of HO8910 and A2780 cells overexpressing Lnc-DARS-AS1 were measured by transwell assay. (f) MTT assays were used to detect the proliferation of HO8910 and A2780 cells overexpressing Lnc-DARS-AS1. (g) The expression levels of epithelial-mesenchymal transition (EMT)-related proteins in HO8910 and A2780 cells overexpressing Lnc-DARS-AS1 were detected by western blot assay. All experiments were repeated three times. *p<0.05, **p<0.01.

3.3 Malignant phenotypes of ovarian cancer cells upregulated by Lnc-DARS-AS1-upregulated SLC2A12

To investigate the target of Lnc-DARS-AS1 in ovarian cancers, RNA sequencing analysis was performed to screen downstream targets of Lnc-DARS-AS1. The mRNA levels in HO8910 cells transfected with the Lnc-DARS-AS1 overexpression plasmid or the empty vector were analyzed. A total of 143 DEGs were identified in these cells, with 57 downregulated and 86 upregulated genes (Figs. 3a–3c). These DEGs showed enrichment in biological processes related to the regulation of multi-organism processes, as well as in the Influenza A and Herpes simplex infection signaling pathways (Figs. 3d and 3e). Among these DEGs, the top 10 most significantly dysregulated genes were verified by qRT-PCR assay in HO8910 cells overexpressing Lnc-DARS-AS1. Only SLC2A12 levels exhibited a dramatic alteration after overexpressing Lnc-DARS-AS1 (Fig. 3f), which was further supported by the results of the western blot (WB) assay (Fig. 4a). These findings suggest that SLC2A12 may be related to Lnc-DARS-AS1. Furthermore, bioinformatics analysis revealed a binding site between SLC2A12 and Lnc-DARS-AS1 (Fig. 4b). Analysis using R software revealed that SLC2A12 expression was markedly elevated in ovarian cancer tissues compared to normal tissues (Fig. 4c). Additionally, an inverse relationship was found between SLC2A12 levels and overall survival in patients with ovarian cancer (Fig. 4d).

To investigate the function of SLC2A12 in ovarian cancer, we overexpressed SLC2A12 in HO8910 and A2780 cells, and qRT-PCR and WB assays were used for the verification of expression (Fig.e 4e and 4f). In the transwell assay, we observed that the migration and invasion capabilities of HO8910 and A2780 cells overexpressing SLC2A12 were notably enhanced (Fig. 4g). Meanwhile, cell proliferation was also promoted by SLC2A12 overexpression in both HO8910 and A2780 cells (Fig. 4h). Moreover, SLC2A12 overexpression induced the expression of N-cadherin, vimentin, MMP2, and MMP9 in both HO8910 and A2780 cells (Fig. 4i). However, E-cadherin expression was decreased in both cell lines. Collectively, these results demonstrate that SLC2A12 may function as a downstream target of Lnc-DARS-AS1 to enhance the malignant phenotype of ovarian cancer cells.

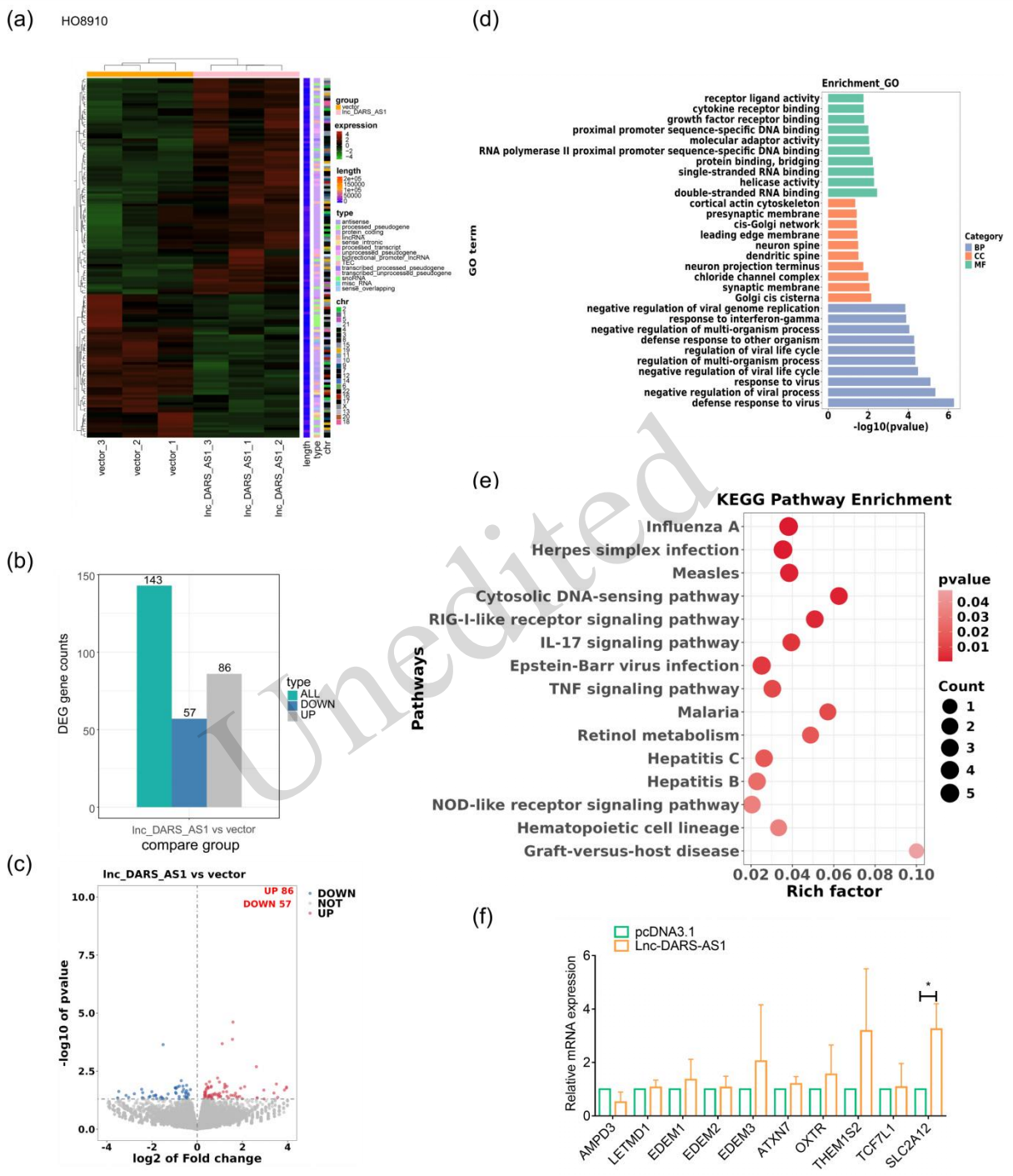

Fig. 3 RNA sequencing analysis of HO8910 cells with Lnc-DARS-AS1 overexpression. The differentially expressed genes (DEGs) in HO8910 cells transfected with Lnc-DARS-AS1 overexpression plasmids are presented as a heatmap (a), a histogram (b), and a volcano plot (c). (d) Gene Ontology (GO) and (e) Kyoto Encyclopedia of Genes and Genomes (KEGG) enrichment analysis were performed on the DEGs. (f) The top 10 DEGs were confirmed by qRT-PCR assay. 'Vector' indicates cells transfected with an empty plasmid (control), while 'DARS-AS1' represents cells transfected with a Lnc-DARS-AS1 overexpression plasmid. The numbers indicate independent biological replicates. *p<0.05.

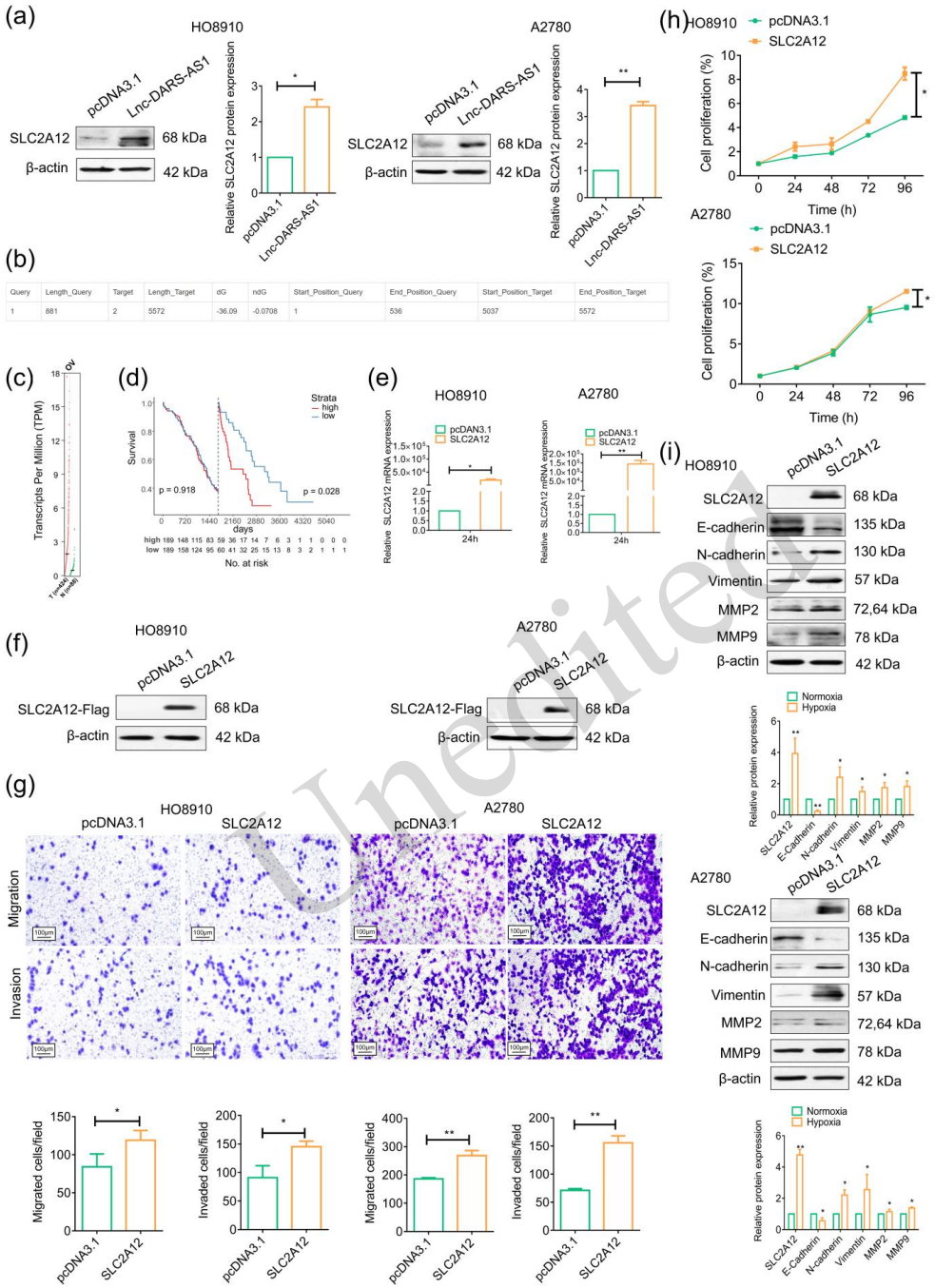

Fig. 4 Role of Lnc-DARS-AS1-regulated SLC2A12 in the malignant phenotype of ovarian cancer cells. (a) The expression of SLC2A12 in ovarian cancer cells overexpressing Lnc-DARS-AS1 was detected by western blot assay. (b) The binding site between SLC2A12 and Lnc-DARS-AS1 was predicted using starBase analysis (https://rnasysu.com/encori/index.php). (c) The expression of SLC2A12 in ovarian cancer tissues was analyzed using R software. (d) The Cancer Genome Atlas (TCGA) database was used to analyze survival curves based on SLC2A12 expression in individuals with ovarian cancer. (e) The expression of SLC2A12 in ovarian cancer cells overexpressing SLC2A12 was detected by quantitative real-time PCR (qRT-PCR). (f) The levels of expression in ovarian cancer cells overexpressing SLC2A12 was detected by western blot assay. (g) The migration and invasion capabilities of HO8910 and A2780 cells overexpressing SLC2A12 were assessed. (h) The proliferation abilities of HO8910 and A2780 cells overexpressing SLC2A12 were measured by MTT assay. (i) The expression levels of epithelial-mesenchymal transition (EMT)-related factors in HO8910 and A2780 cells overexpressing SLC2A12 were measured by western blot assays. All experiments were repeated three times. *p<0.05, **p<0.01.

3.4 The expression of SLC2A12 enhanced by Lnc-DARS-AS1 via competitive binding to miR-378a-5p

Based on the above findings, we determined that Lnc-DARS-AS1 increases the expression of SLC2A12. To investigate the underlying regulatory mechanism, we performed a comprehensive bioinformatics analysis to identify miRNAs potentially targeting both molecules. Differential expression analysis of the GSE261800 dataset identified 166 significantly dysregulated miRNAs in ovarian cancer and adjacent normal samples. Intersection analysis between these differentially expressed miRNAs and 190 SLC2A12-targeting miRNAs predicted by miRDB revealed 14 candidates, as shown in the Venn diagram (Fig. 5a). Subsequent validation in the GSE261800 dataset confirmed that hsa-miR-378a-5p was significantly downregulated in ovarian cancer samples compared to normal tissues (Fig. 5b), suggesting its potential role as a tumor suppressor. This miRNA had not been previously reported to link Lnc-DARS-AS1 and SLC2A12 in ovarian cancer. Among these candidates, hsa-miR-378a-5p was selected for further investigation based on this bioinformatics evidence. To confirm the function of miR-378a-5p, we transfected HO8910 and A2780 cells with a miR-378a-5p mimic. After transfecting HO8910 and A2780 cells with miR-378a-5p mimics and their negative controls for 24 and 48 h, the expression levels of miR-378a-5p, Lnc-DARS-AS1, and SLC2A12 were detected by qRT-PCR. The results showed that miR-378a-5p mimics successfully increased miR-378a-5p expression while decreasing the expression of Lnc-DARS-AS1 and SLC2A12 in HO8910 and A2780 cells (Fig. 5c). Further analysis confirmed that cells overexpressing Lnc-DARS-AS1 showed the increased expression of SLC2A12. However, miR-378a-5p mimics suppressed the Lnc-DARS-AS1-induced upregulation of SLC2A12 at the protein level (Fig. 5d).

To verify the binding relationship among SLC2A12, Lnc-DARS-AS1, and miR-378a-5p, wild-type and mutant SLC2A12 or Lnc-DARS-AS1 carried on luciferase reporter plasmids were transfected into HO8910 cells. The luciferase activity of the reporter plasmid containing the wild-type SLC2A12 3'-UTR was significantly increased in HO8910 cells overexpressing Lnc-DARS-AS1 compared to that in cells transfected with the corresponding control (Fig. 6a). Compared to the control, the luciferase activity of wild-type SLC2A12 was notably reduced in HO8910 cells transfected with the miR-378a-5p mimic, while that of mutant-type SLC2A12 showed no change, suggesting that miR-378a-5p may bind to the 3’UTR region of SLC2A12 mRNA (Fig. 6b). Moreover, after co-transfecting HO8910 cells with miR-378a-5p mimics or their negative control, Lnc-DARS-AS1 plasmid or their control, and wild-type SLC2A12 3’UTR luciferase reporter plasmid or their control for 24 h, dual-luciferase reporter assay demonstrated that Lnc-DARS-AS1 promoted SLC2A12 expression, while miR-378a-5p counteracted this effect (Fig. 6c). Similarly, the luciferase activity of wild-type Lnc-DARS-AS1 was markedly decreased in HO8910 cells overexpressing miR-378a-5p compared to that in control cells, while that of mutant-type Lnc-DARS-AS1 was not affected by miR-378a-5p mimics (Fig. 6d). In summary, these observations provide evidence for direct binding among Lnc-DARS-AS1, miR-378a-5p and SLC2A12. To further elucidate the regulatory mechanism, we found that the overexpression of Lnc-DARS-AS1 led to a significant upregulation of miR-378a-5p expression (Fig. 6e). Subsequent biotin-labeled miRNA pull-down assays confirmed the direct and substantial binding between Lnc-DARS-AS1 and miR-378a-5p, as demonstrated by the significant enrichment of Lnc-DARS-AS1 (Fig. 6f). Notably, under the same experimental conditions, no significant enrichment of SLC2A12 was observed (Fig. 6f), indicating that while both molecules are targets of miR-378a-5p, their binding affinities may differ. This suggests that Lnc-DARS-AS1, acting as a ceRNA, competitively binds to miR-378a-5p to increase the expression of SLC2A12.

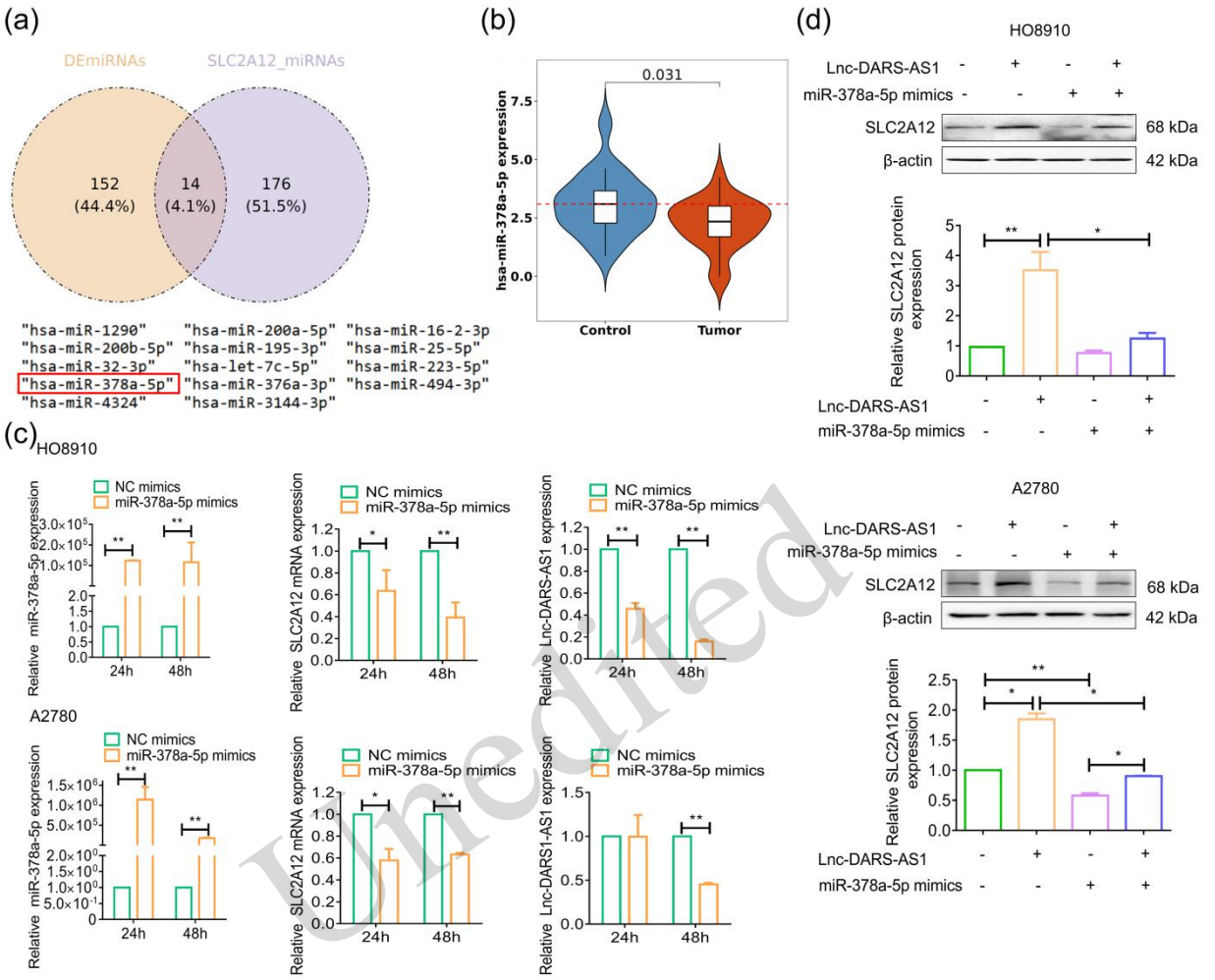

Fig. 5 Regulation of SLC2A12 by Lnc-DARS-AS1 and miR-378a-5p. (a) A Venn diagram was used to show the intersection between dysregulated miRNAs in ovarian cancer and adjacent normal samples and SLC2A12-targeting miRNAs predicted by miRDB. (b) The Wilcoxon test was used to determine the expression of hsa-miR-378a-5p in ovarian cancer versus adjacent tissues from the GSE261800 dataset. (c) The mRNA expression levels of miR-378a-5p, SLC2A12, and Lnc-DARS-AS1 were examined in HO8910 and A2780 cells transfected with miR-378a-5p mimics. (d) The protein expression level of SLC2A12 was measured in HO8910 and A2780 cells co-transfected with plasmids overexpressing Lnc-DARS-AS1 and miR-378a-5p mimics. All experiments were repeated three times. *p<0.05, **p<0.01.

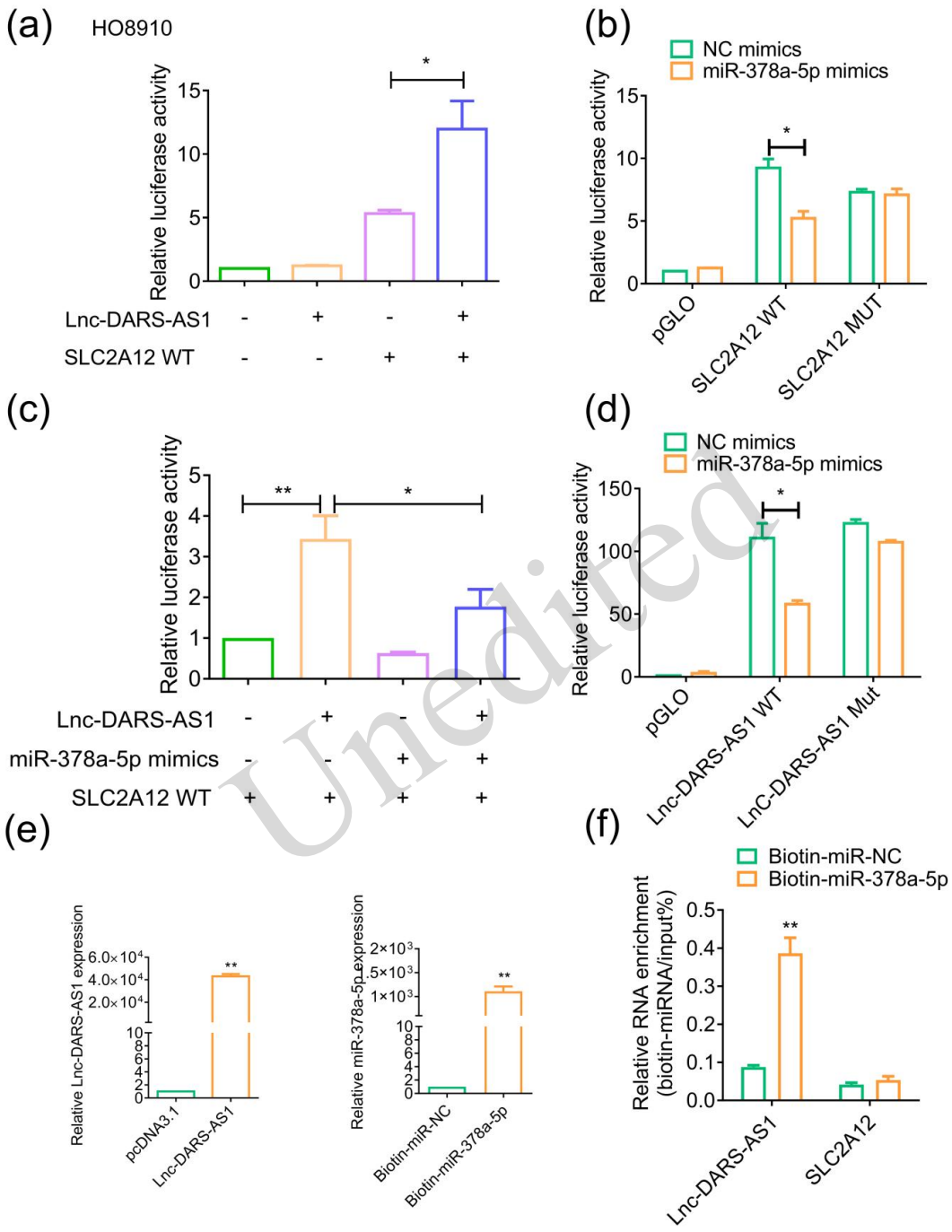

Fig. 6 Interaction among Lnc-DARS-AS1, miR-378a-5p, and SLC2A12. (a) Luciferase activity was detected in HO8910 cells co-transfected with plasmids overexpressing Lnc-DARS-AS1 and SLC2A12-WT. (b) Luciferase activity was measured in SLC2A12-WT or SLC2A12-MUT HO8910 cells transfected with miR-378a-5p mimics. (c) Luciferase activity was detected in HO8910 cells overexpressing Lnc-DARS-AS1 co-transfected with miR-378a-5p mimics, and SLC2A12-WT plasmids. (d) Luciferase activity in HO8910 cells overexpressing miR-378a-5p co-transfected with Lnc-DARS-AS1-WT or Lnc-DARS-AS1-MUT was detected. (e) mRNA expression levels of miR-378a-5p and Lnc-DARS-AS1 were examined in HO8910 cells transfected with Lnc-DARS-AS1 overexpression plasmids. (f) Biotin-labeled miRNA pull-down assays were used to evaluate the binding between Lnc-DARS-AS1, SLC2A12, and miR-378a-5p. All experiments were repeated three times. *p<0.05, **p<0.01.

3.5 The malignant phenotypes of ovarian cancer cells promoted by hypoxia-derived Lnc-DARS-AS1 via the Lnc-DARS-AS1/miR-378a-5p/SLC2A12 axis

To further determine whether hypoxia-derived Lnc-DARS-AS1 is involved in ovarian cancer progression via the Lnc-DARS-AS1/miR-378a-5p/SLC2A12 axis, two siRNAs targeting SLC2A12 were designed, and the results showed that transfection with siR-SLC2A12-2 for 24 h achieved a higher knockdown efficiency in both HO8910 and A2780 cells (Figs. 7a and S1a). Subsequently, HO8910 and A2780 cells were co-transfected with siR-SLC2A12-2 or negative control (NC), cultured under hypoxic conditions for 24 h. Then, their migratory and invasive abilities were assessed using a transwell assay (Figs. 7b and S1b). As expected, silencing SLC2A12 expression significantly reversed the hypoxia-induced enhancement of cell migration and invasion. Next, siR-Lnc-DARS-AS1 was employed to assess the impact of Lnc-DARS-AS1 on ovarian cancer cells under hypoxic conditions. The silencing effect of Lnc-DARS-AS1 was assessed by qRT-PCR (Figs. 7c and S1c), and siR-Lnc-DARS-AS1-2 was used in subsequent experiments. HO8910 and A2780 cells were transfected with siR-Lnc-DARS-AS1 and cultured under hypoxic conditions for 24 h. The results showed that siR-Lnc-DARS-AS1 suppressed hypoxia-induced SLC2A12 expression at the protein level (Figs. 7d and S1d). The transwell assay results showed that the migratory and invasive abilities of cells under hypoxic conditions were reduced following Lnc-DARS-AS1 silencing (Figs. 7e and S1e).

Furthermore, HO8910 cells were co-transfected with an Lnc-DARS-AS1 overexpression plasmid and SLC2A12 siRNA for 24 h (Fig 8a). The transwell assay results showed that SLC2A12 silencing significantly reversed the enhancement of cell migration and invasion induced by Lnc-DARS-AS1 overexpression. Next, HO8910 cells were co-transfected with an SLC2A12 overexpression plasmid and miR-378a-5p mimics for 24 h to perform gain- and loss-of-function experiments (Fig. 8b). As anticipated, cellular function experiments demonstrated that high SLC2A12 expression significantly enhanced the metastatic ability of ovarian cancer cells, whereas miR-378a-5p mimics reversed this effect (Figs. 8c and 8d). In addition, clinical tissue samples from primary and metastatic lesions of 20 patients with ovarian cancer were analyzed. As shown in Fig. 8e, the metastatic lesions displayed more necrotic regions compared to the primary lesions. There was a marked increase in SLC2A12 and HIF-1α expression in metastatic lesions, supporting the role of SLC2A12 in facilitating the metastasis of ovarian cancer (Fig. 8f). To further validate these findings on a larger scale, we analyzed data from the TCGA ovarian cancer cohort, which demonstrated a significant correlation between elevated SLC2A12 expression and advanced FIGO disease stages (Table 5). Furthermore, the analysis of the GSE218939 dataset demonstrated a significant positive correlation between SLC2A12 and HIF-1α expression across 22 primary and 29 metastatic ovarian cancer samples (Fig. 8g), providing additional evidence that SLC2A12 expression is associated with hypoxia response. Collectively, our findings indicate that hypoxia-derived Lnc-DARS-AS1 promotes ovarian cancer progression via the Lnc-DARS-AS1/miR-378a-5p/SLC2A12 axis.

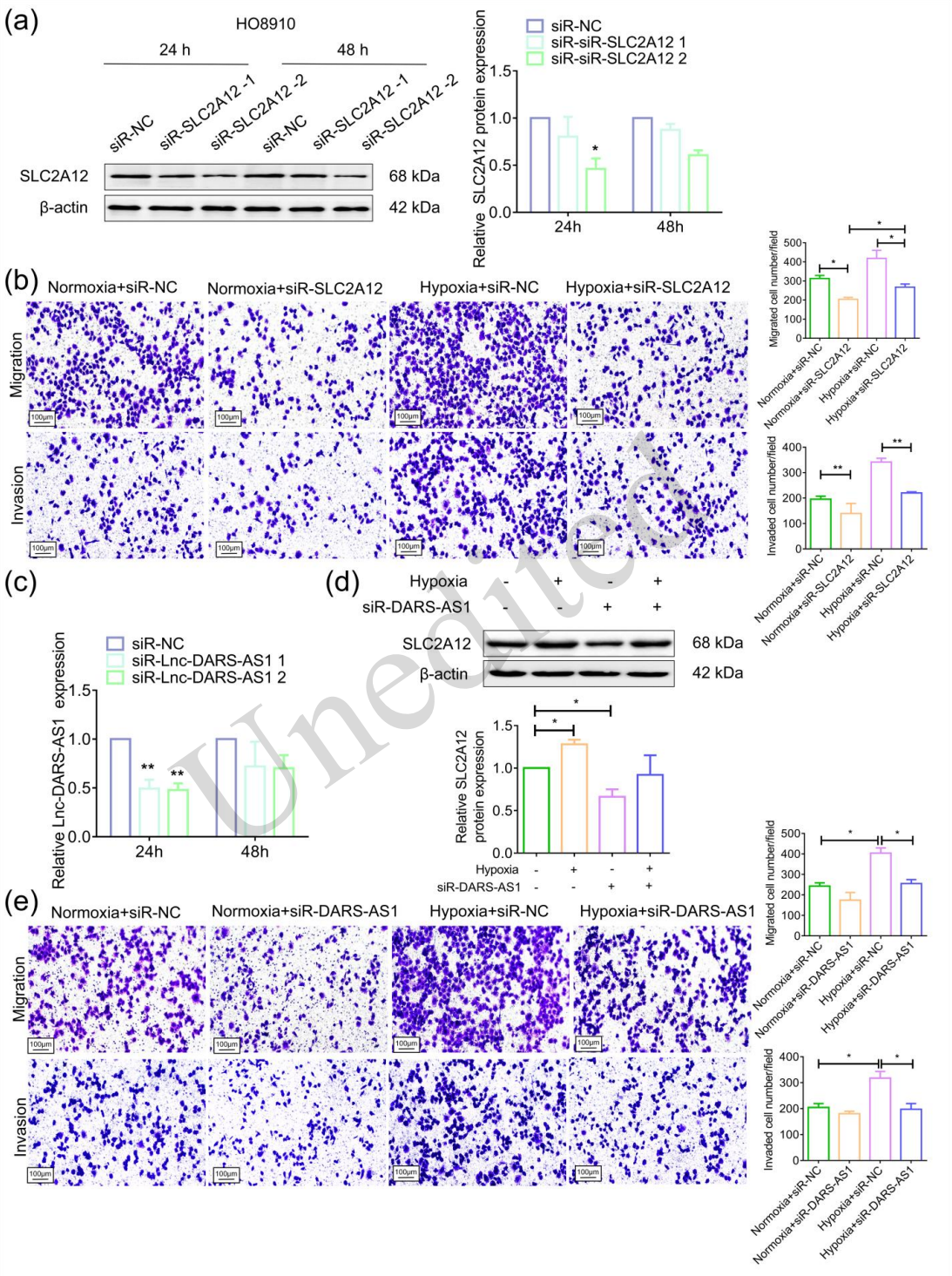

Fig. 7 Promotion of malignant phenotype by Lnc-DARS-AS1 via SLC2A12 in HO8910 cells. (a) The knockdown efficiency of SLC2A12 was examined by western blot assay. (b) The invasiveness and migratory ability of SLC2A12-silenced HO8910 cells were examined under normoxic or hypoxic conditions. (c) Quantitative real-time PCR (qRT-PCR) was used to examine the knockdown efficiency of Lnc-DARS-AS1. (d) A western blot assay was used to detect the expression of SLC2A12. (e) The invasiveness and migratory ability of Lnc-DARS-AS1-silenced HO8910 cells were examined under normoxic or hypoxic conditions. All experiments were repeated three times. *p<0.05, **p<0.01.

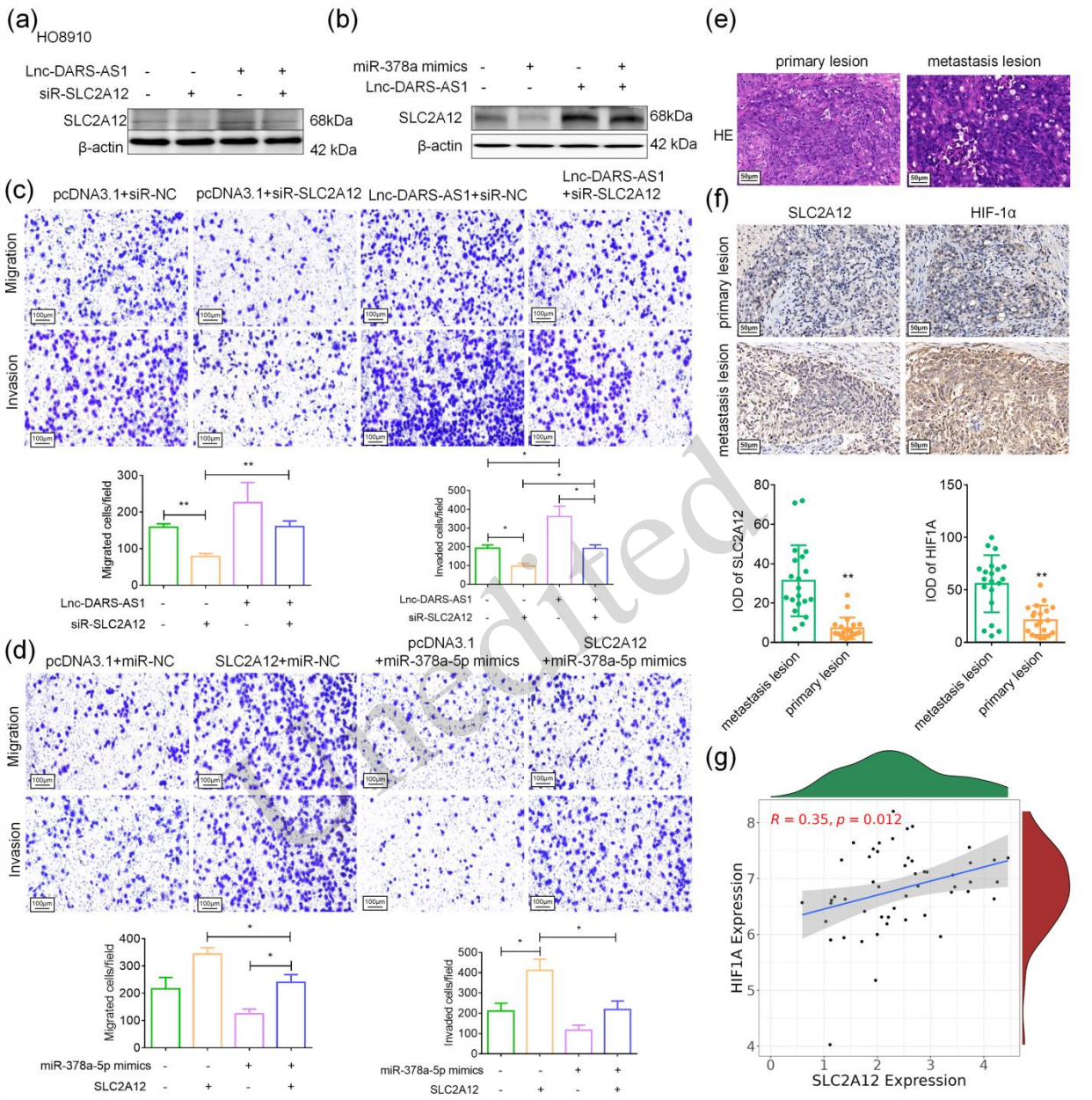

Fig. 8 Role of the Lnc-DARS-AS1/miR-378a-5p/SLC2A12 axis in promoting malignant phenotype in HO8910 cells. (a) The expression of SLC2A12 was measured in HO8910 cells co-transfected with Lnc-DARS-AS1 overexpression plasmids and SLC2A12-silencing plasmids. (b) The expression of SLC2A12 was measured in HO8910 cells co-transfected with Lnc-DARS-AS1 overexpression plasmids and miR-378a-5p mimic plasmids. (c) The invasiveness and migratory ability were measured in HO8910 cells co-transfected with Lnc-DARS-AS1 overexpression plasmids and SLC2A12 silencing plasmids. (d) The invasiveness and migratory ability were measured in HO8910 cells co-transfected with Lnc-DARS-AS1 overexpression plasmids and miR-378a-5p mimic plasmids. (e) Hematoxylin-eosin (HE) staining was performed on primary and metastatic lesions. (f) The expressions of SLC2A12 and HIF-1α were examined via immunohistochemistry assays. (g) The correlation between SLC2A12 and HIF-1α was evaluated by constructing scatter plots using the ggpubr package. All experiments were repeated three times. *p<0.05, **p<0.01.

Table 5 Clinical relevance analysis of the SLC2A12 gene

Characteristic	Category	High expression of SLC2A12	Low expression of SLC2A12	*P*
Age	≤65	102 (49.5)	127 (61.1)	0.024
	>65	104 (50.5)	81 (38.9)	
Race	non-White	31 (15.0)	16 (7.7)	0.028
	White	175 (85.0)	192 (92.3)	
Stage	Stage I/II/IIIA/IIIB (Low Burden)	33 (16.0)	16 (7.7)	
	Stage IIIC	141 (68.4)	161 (77.4)	0.027
	Stage IV	32 (15.5)	31 (14.9)	

4 Discussion

Ovarian cancer has a high metastatic rate, posing a major threat to the health of affected women worldwide (Yang et al., 2022). Patients with recurrent platinum-resistant ovarian cancer face a poor prognosis and limited treatment options (Havasi et al., 2023). Interactions between tumor cells and the TME contribute to the complex process of platinum treatment resistance. Gonçalves et al. (Goncalves, et al., 2021) reported that tumor cells undergo metabolic reprogramming, with high metabolic flexibility associated with the TME. Therefore, it is essential to understand the molecular mechanisms underlying the TME-mediated intratumoral metabolic heterogeneity. Furthermore, clarifying the progression of ovarian cancer and identifying new therapeutic targets have become urgent priorities.

Hypoxia in the tumor microenvironment is a well-established characteristic of solid tumors, occurring in approximately 90% of cases (Godet et al., 2019). Increasing evidence suggests that hypoxia leads to the metabolic reprogramming of cancer cells, thereby accelerating metastasis (Paredes et al., 2021). More significantly, cancer cells exhibit increased invasiveness and drug resistance after adaptation to hypoxia (Jing et al., 2019). HIF-1α-induced glycolytic metabolism increases cisplatin resistance in ovarian cancer, involving the production of reactive oxygen species (Ai et al., 2016). Therefore, further investigations into the relationship between hypoxia and cancer are required. The increase in HIF-1α expression under hypoxia is a well-documented phenomenon. By regulating the expression of downstream target genes, HIF-1α (a transcription factor with a broad range of target genes) can affect intracellular protein levels (Huang et al., 2017; Wicks and Semenza, 2022). Furthermore, alterations in the cancer and stromal cells within the TME promote cancer invasiveness. The association between EMT and hypoxia has been investigated extensively (Saxena et al., 2020). EMT is characterized by reduced intercellular adhesion and the increased expression of mesenchymal markers. Previous studies have demonstrated that EMT is associated with cancer cell migration, stemness and drug resistance (Jolly et al., 2015). Our data revealed that hypoxia leads to decreased levels of E-cadherin in ovarian cancer cells but increased expression levels of N-cadherin, vimentin, MMP2, and MMP9. This indicates that hypoxia promotes the mesenchymal phenotype of ovarian cancer cells, which is in agreement with the results reported by Tsutomu et al. (Imai et al., 2003).

Our study systematically elucidated a novel molecular pathway through which hypoxia drives the malignant progression of ovarian cancer. First, we confirmed that hypoxia itself is a potent driver of malignancy

in ovarian cancer cells. Exposure to hypoxic conditions significantly enhanced the migratory and invasive capabilities of HO8910 and A2780 cells, consistent with the established role of hypoxia in promoting metastasis. Notably, we observed a concomitant decrease in cell proliferation. The molecular hallmarks of hypoxia were confirmed by the robust upregulation of HIF-1α. Furthermore, hypoxia induced a clear EMT, as evidenced by the characteristic shift in marker expression: the downregulation of E-cadherin and the upregulation of N-cadherin, vimentin, and the matrix metalloproteinases MMP2 and MMP9.

Recent studies have indicated that lncRNAs and miRNAs are involved in hypoxia-mediated tumor EMT in various cancers, including ovarian cancer (Xu et al., 2016; Ang et al., 2023). As described in the literature, lncRNA transcription is closely related to mRNA expression via RNA polymerase II (Peng et al., 2021). Interestingly, the function of lncRNAs depends on their specific location, with epigenetic regulation occurring in the cell nucleus, and protein stabilization and miRNA sequestration taking place in the cytoplasm. Furthermore, lncRNAs present in exosomes function as signaling molecules, therefore the identification of appropriate lncRNAs may contribute to the discovery of new therapeutic targets for hypoxia-related cancers. In this study, through lncRNA sequencing analysis, we found significant changes in Lnc-DARS-AS1. Overexpression of DARS-AS1 has been detected in various cancers (Shu et al., 2024). For instance, miR-330-3p is regulated by DARS-AS1, leading to increased NAT10 expression and gastric cancer cell proliferation (Du et al., 2022). In addition, the inhibition of DARS-AS1 attenuates the progression of cervical cancer (Zhu and Han, 2021). DARS-AS1 regulates miR-194-5p and promotes oncogenic effects in ovarian cancer by acting as an miRNA sponge, thereby regulating the expression of RBX1 to inhibit TP53 ubiquitination and degradation (Zhou et al., 2021). Notably, it has been reported that hypoxia induces DARS-AS1 expression in a HIF-1α-dependent manner, contributing to multiple myeloma progression through the HIF-1/DARS-AS1/RBM39 axis (Tong et al., 2020). Similarly, under hypoxic conditions, DARS-AS1 was shown to be upregulated in renal tubular cells, highlighting its role as a hypoxia-responsive lncRNA beyond cancer contexts (Mimura et al., 2017). Based on this established regulatory background, we further investigated the functional role and molecular mechanisms of DARS-AS1 in ovarian cancer, with particular focus on its potential as a ceRNA under hypoxic conditions. Functional experiments established Lnc-DARS-AS1 as a key oncogenic driver. Its overexpression was sufficient to recapitulate the hypoxic phenotype, enhancing cell migration, invasion, proliferation, and EMT. This positions Lnc-DARS-AS1 as a critical downstream effector of hypoxia-induced signaling. We next sought to identify the mechanism by which Lnc-DARS-AS1 exerts its effects. RNA sequencing subsequent to Lnc-DARS-AS1 overexpression revealed SLC2A12 as its most significantly upregulated target gene, and bioinformatics analysis predicted that this interaction is direct. Clinically, SLC2A12 expression was not only elevated in ovarian cancer tissues but also correlated with advanced disease stage and poorer patient survival, underscoring its pathological relevance. Mirroring the effects of Lnc-DARS-AS1, the overexpression of SLC2A12 markedly enhanced cell migration, invasion, proliferation, and EMT *in vitro*, confirming its role as a functional mediator of the oncogenic role of Lnc-DARS-AS1.

SLC2A12 belongs to the SLC2 family. There is evidence that SLC2A12 contributes to cancer development and is a potential therapeutic target for gastric cancer (Sexton et al., 2020). In prostate cancer, SLC2A12 has been associated with androgen receptors and encodes GLUT12 (White et al., 2018). Li et al. (Li et al., 2023) found that SLC2A12 is highly expressed in hypoxic ovarian cancer cells and is related to glutathione and lipid metabolism, thereby inhibiting ferroptosis in ovarian cancer cells. In hypoxic ovarian cancer cells, SLC2A12 (GLUT12)—a hypoxia-upregulated glucose transporter (Burgos et al., 2025)—drives proliferation and EMT, probably via affecting glucose metabolism. It enhances glucose uptake to fuel the Warburg effect (aerobic glycolysis), a metabolic shift that prioritizes biomass synthesis (nucleotides, lipids) over efficient ATP production and is critical for supporting cell division (Vander Heiden et al., 2009). This aligns with findings in other types of cancer, where SLC2A12 overexpression boosts glycolysis and cell growth (Shi et al., 2020; Cao et al., 2023). For EMT induction, SLC2A12-mediated glycolysis diverts intermediates to the hexosamine biosynthetic pathway (HBP), generating uridine diphosphate N-acetylglucosamine (UDP-GlcNAc). This

metabolite drives the O-GlcNAcylation of EMT regulators (e.g., Snail, β-catenin), stabilizing these factors to promote mesenchymal marker expression (Taparra et al., 2016). Though specific data on ovarian cancer is limited, the role of SLC2A12 in the enhancement of cancer cell migration/invasion (Shi, et al., 2020) supports its EMT-promoting function in hypoxia. Clinically, SLC2A12 overexpression correlates with poor prognosis in solid tumors (Burgos, et al., 2025), underscoring its relevance as a metabolic node linking hypoxia to ovarian cancer progression.

The regulatory mechanism connecting these molecules was revealed to be a ceRNA network. Bioinformatics analysis and molecular validation identified miR-378a-5p as a shared target of both Lnc-DARS-AS1 and SLC2A12. We confirmed that miR-378a-5p acts as a tumor suppressor: its expression is downregulated in clinical samples, and its overexpression can suppress the expression of both Lnc-DARS-AS1 and SLC2A12. A series of luciferase reporter assays confirmed the direct binding relationships: miR-378a-5p binds to the 3' untranslated regions (3'UTRs) of both SLC2A12 and Lnc-DARS-AS1, and Lnc-DARS-AS1 can sequester miR-378a-5p, thereby relieving its repressive effect on SLC2A12. Crucially, a biotin-labeled miRNA pull-down assay provided direct evidence for the physical binding between Lnc-DARS-AS1 and miR-378a-5p.

MiR-378a-5p, encoded by *PPARGC1B*, is recognized as an independent prognostic marker for tumors (Qin et al., 2022). Target protein translation can be obstructed by miRNAs through cleavage or binding to the 3’UTR of the corresponding mRNA (He and Hannon, 2004). Although there are no previous reports on the role of miR-378-5p in ovarian cancer, that of miR-378-3p (a member of the miR-378a family) in this type of cancer has been established. The upregulation of GALNT3 expression by Lnc-PSMA3-AS1 through competitive binding with miR-378-3p accelerates ovarian cancer growth (Xu et al., 2021). The function of miR-378a is still a subject of controversy, given that high miR-378a expression was associated with unfavorable outcomes in patients with cholangiocarcinoma (Zhou and Ma, 2019). Our study revealed that miR-378a-5p exerts anti-oncogenic effects in ovarian cancer, offering fresh perspectives on the function of miR-378a in cancer.

Finally, rescue experiments confirmed the physiological relevance of this entire axis within the context of hypoxia: the knockdown of either Lnc-DARS-AS1 or SLC2A12 effectively attenuated the pro-migratory and pro-invasive effects of hypoxia. Importantly, the oncogenic effects of Lnc-DARS-AS1 overexpression were suppressed by the co-knockdown of SLC2A12. Similarly, the effects of SLC2A12 overexpression were reversed by miR-378a-5p mimics, confirming the linear dependency of this pathway. The clinical correlation between SLC2A12, HIF-1α, and metastasis provides compelling translational evidence that this hypoxia-driven Lnc-DARS-AS1/miR-378a-5p/SLC2A12 axis is operational in human ovarian cancer progression.

Our findings revealed that the Lnc-DARS-AS1/miR-378a-5p/SLC2A12 axis represents a mechanistically distinct pathway from previously established hypoxia-induced mechanisms in ovarian cancer. While canonical HIF-1α signaling primarily regulates the transcriptional activation of genes involved in angiogenesis (Zhang et al., 2024), glycolysis (Sun et al., 2019), and glucose transport-related genes (Seeber, et al., 2011), the axis identified in the present study operates through the post-transcriptional regulation of a different glucose transporter isoform. This pathway is particularly significant given the unique kinetic properties and insulin sensitivity of SLC2A12 (Rogers et al., 2002; Xiong and Lei, 2021), suggesting a previously unrecognized layer of metabolic regulation in the tumor microenvironment. Furthermore, unlike other lncRNAs that regulate the hypoxia response through angiogenesis or the regulation of apoptosis (Shu et al., 2020; Gao et al., 2022), Lnc-DARS-AS1 specifically fine-tunes metabolic adaptation through ceRNA mechanisms. This discovery expands the repertoire of hypoxia response strategies available to ovarian cancer cells and highlights the complexity of metabolic reprogramming in the TME.

This study has several limitations that should be acknowledged. First, although the use of public datasets such as TCGA and GEO strengthens the statistical support for our conclusions, the retrospective nature of these databases introduces inherent selection biases that must be considered. Second, we recognize the limitation regarding the use of the HO8910 cell line, which has been identified in the Cellosaurus database as a potentially misidentified cell line due to HeLa cell contamination. However, all key experiments and conclusions presented in this study were consistently validated for the A2780 ovarian cancer cell line, which is a well-characterized

and authenticated ovarian cancer model without any known contamination issues. This parallel verification across multiple cell models improves the reliability of our findings despite this limitation. Furthermore, as this work explored novel biomarkers in ovarian cancer, including Lnc-DARS-AS1 and miR-378a-5p, further validation in relevant animal models is essential before advancing to larger clinical studies. Future research should focus on expanding prospective clinical cohorts across diverse populations to validate the prognostic value of this axis, establishing physiologically relevant animal models to investigate its functional mechanisms *in vivo* and exploring potential clinical applications through targeted therapeutic strategies.

5 Conclusions

Our study revealed for the first time that hypoxia-induced Lnc-DARS-AS1 promotes the progression of ovarian cancer through the Lnc-DARS-AS1/miR-378a-5p/SLC2A12 axis. Considering its role in the modulation of cancer cell migration and invasiveness, targeting this axis may offer a novel approach to treatment, particularly in cases characterized by resistance to conventional therapies. To assess the broader applicability of our results, future studies should aim to validate these findings in diverse patient populations and explore similar pathways in other types of cancer.

Data availability statement

All data generated or analyzed during this study are included in this published article (and its supplementary information files). The raw datasets are available from the corresponding author upon reasonable request.

Acknowledgments

We are grateful to Dr. Li Yang and Editage for English language editing. This work was supported by the National Natural Science Foundation of China [grant number 81703748], and partly supported by the Medical Science and Technology Foundation of Zhejiang Province [grant number 2023KY060, 2024KY714] and the Zhejiang Province Traditional Chinese Medicine Science and Technology Project [grant number 2024ZL277].

Author contributions

Wenjie ZENG: Conceptualization, Formal analysis, Funding acquisition and Writing - original draft; Hubin XU, Haimin JIANG and Mengyu ZHANG: Methodology, Validation, Software; Huafeng SHOU and Xiaoyan CHEN: Software, Data curation, Project administration; Weiguo LU: Conceptualization, Writing review and editing, Validation, Supervision. All authors read and approved the final manuscript.

Compliance with ethics guidelines

Wenjie ZENG, Hubin XU, Haimin JIANG, Mengyu ZHANG, Huafeng SHOU, Xiaoyan CHEN, and Weiguo LU declare that they have no conflict of interest. All authors (Wenjie ZENG, Hubin XU, Haimin JIANG, Mengyu ZHANG, Huafeng SHOU, Xiaoyan CHEN, and Weiguo LU) confirm the absence of any financial or non-financial interests that could be construed as influencing the research.

All procedures involving human participants were performed in accordance with the ethical standards of the Ethics Committee of Zhejiang Provincial People's Hospital and with the 1964 Helsinki Declaration and its later amendments (2008 revision). The study protocol was approved by the Ethics Committee of Zhejiang Provincial People's Hospital (Approval No. 2025021). Informed consent was obtained from all individual participants included in the study.

References

Abildgaard C, Do Canto LM, Steffensen KD, et al., 2019. Long non-coding rnas involved in resistance to chemotherapy in ovarian cancer. Front Oncol, 9:1549.

https://doi.org/10.3389/fonc.2019.01549
Ai Z, Lu Y, Qiu S, et al., 2016. Overcoming cisplatin resistance of ovarian cancer cells by targeting hif-1-regulated cancer metabolism. *Cancer Lett*, 373(1):36-44.
https://doi.org/10.1016/j.canlet.2016.01.009
Ang HL, Mohan CD, Shanmugam MK, et al., 2023. Mechanism of epithelial-mesenchymal transition in cancer and its regulation by natural compounds. *Med Res Rev*, 43(4):1141-1200.
https://doi.org/10.1002/med.21948
Armstrong DK, Alvarez RD, Backes FJ, et al., 2022. Nccn guidelines(r) insights: Ovarian cancer, version 3.2022. *J Natl Compr Canc Netw*, 20(9):972-980.
https://doi.org/10.6004/jnccn.2022.0047
Braga EA, Fridman MV, Moscovtsev AA, et al., 2020. Lncrnas in ovarian cancer progression, metastasis, and main pathways: Cerna and alternative mechanisms. *Int J Mol Sci*, 21(22)
https://doi.org/10.3390/ijms21228855
Burgos M, Gil-Iturbe E, Idoate-Bayon A, et al., 2025. The glucose transporter glut12, a new actor in obesity and cancer. *J Physiol Biochem*, 81(2):391-401.
https://doi.org/10.1007/s13105-024-01028-9
Cao B, Zhao R, Li H, et al., 2023. Inhibition of androgen receptor enhanced the anticancer effects of everolimus through targeting glucose transporter 12. *Int J Biol Sci*, 19(1):104-119.
https://doi.org/10.7150/ijbs.75106
Chandra A, Pius C, Nabeel M, et al., 2019. Ovarian cancer: Current status and strategies for improving therapeutic outcomes. *Cancer Med*, 8(16):7018-7031.
https://doi.org/10.1002/cam4.2560
Colombo I, Karakasis K, Suku S, et al., 2023. Chasing immune checkpoint inhibitors in ovarian cancer: Novel combinations and biomarker discovery. *Cancers (Basel)*, 15(12)
https://doi.org/10.3390/cancers15123220
Du C, Han X, Zhang Y, et al., 2022. Dars-as1 modulates cell proliferation and migration of gastric cancer cells by regulating mir-330-3p/nat10 axis. *Open Med (Wars)*, 17(1):2036-2045.
https://doi.org/10.1515/med-2022-0583
Gao L, Yang J, Li Y, et al., 2022. Long noncoding rna scirt promotes huvec angiogenesis via stabilizing vegfa mrna induced by hypoxia. *Oxid Med Cell Longev*, 2022:9102978.
https://doi.org/10.1155/2022/9102978
Godet I, Shin YJ, Ju JA, et al., 2019. Fate-mapping post-hypoxic tumor cells reveals a ros-resistant phenotype that promotes metastasis. *Nat Commun*, 10(1):4862.
https://doi.org/10.1038/s41467-019-12412-1
Goncalves AC, Richiardone E, Jorge J, et al., 2021. Impact of cancer metabolism on therapy resistance - clinical implications. *Drug Resist Updat*, 59:100797.
https://doi.org/10.1016/j.drup.2021.100797
Hashemi M, Moosavi MS, Abed HM, et al., 2022. Long non-coding rna (lncrna) h19 in human cancer: From proliferation and metastasis to therapy. *Pharmacol Res*, 184:106418.
https://doi.org/10.1016/j.phrs.2022.106418
Havasi A, Cainap SS, Havasi AT, et al., 2023. Ovarian cancer-insights into platinum resistance and overcoming it. *Medicina (Kaunas)*, 59(3)
https://doi.org/10.3390/medicina59030544
He L, Hannon GJ, 2004. Micrornas: Small rnas with a big role in gene regulation. *Nat Rev Genet*, 5(7):522-531.
https://doi.org/10.1038/nrg1379
Huang Y, Lin D, Taniguchi CM, 2017. Hypoxia inducible factor (hif) in the tumor microenvironment: Friend or foe? *Sci China Life Sci*, 60(10):1114-1124.
https://doi.org/10.1007/s11427-017-9178-y
Imai T, Horiuchi A, Wang C, et al., 2003. Hypoxia attenuates the expression of e-cadherin via up-regulation of snail in ovarian carcinoma cells. *Am J Pathol*, 163(4):1437-1447.
https://doi.org/10.1016/S0002-9440(10)63501-8
Jiang Y, Wang C, Zhou S, 2020. Targeting tumor microenvironment in ovarian cancer: Premise and promise. *Biochim Biophys Acta Rev Cancer*, 1873(2):188361.
https://doi.org/10.1016/j.bbcan.2020.188361
Jing X, Yang F, Shao C, et al., 2019. Role of hypoxia in cancer therapy by regulating the tumor microenvironment. *Mol Cancer*, 18(1):157.
https://doi.org/10.1186/s12943-019-1089-9
Jolly MK, Boareto M, Huang B, et al., 2015. Implications of the hybrid epithelial/mesenchymal phenotype in metastasis. *Front Oncol*, 5:155.
https://doi.org/10.3389/fonc.2015.00155
Li M, Li L, Cheng X, et al., 2023. Hypoxia promotes the growth and metastasis of ovarian cancer cells by suppressing ferroptosis via upregulating slc2a12. *Exp Cell Res*, 433(2):113851.

https://doi.org/10.1016/j.yexcr.2023.113851
Liu HZ, Liu GY, Pang WW, et al., 2020. Lncrna lucat1 promotes proliferation of ovarian cancer cells by regulating mir-199a-5p expression. *Eur Rev Med Pharmacol Sci*, 24(4):1682-1687.
https://doi.org/10.26355/eurrev_202002_20342
Mccabe EM, Rasmussen TP, 2021. Lncrna involvement in cancer stem cell function and epithelial-mesenchymal transitions. *Semin Cancer Biol*, 75:38-48.
https://doi.org/10.1016/j.semcancer.2020.12.012
Mimura I, Hirakawa Y, Kanki Y, et al., 2017. Novel lnc rna regulated by hif-1 inhibits apoptotic cell death in the renal tubular epithelial cells under hypoxia. *Physiol Rep*, 5(8)
https://doi.org/10.14814/phy2.13203
Paredes F, Williams HC, San Martin A, 2021. Metabolic adaptation in hypoxia and cancer. *Cancer Lett*, 502:133-142.
https://doi.org/10.1016/j.canlet.2020.12.020
Peng PH, Hsu KW, Chieh-Yu Lai J, et al., 2021. The role of hypoxia-induced long noncoding rnas (lncrnas) in tumorigenesis and metastasis. *Biomed J*, 44(5):521-533.
https://doi.org/10.1016/j.bj.2021.03.005
Peng WX, Koirala P, Mo YY, 2017. Lncrna-mediated regulation of cell signaling in cancer. *Oncogene*, 36(41):5661-5667.
https://doi.org/10.1038/onc.2017.184
Qin Y, Liang R, Lu P, et al., 2022. Depicting the implication of mir-378a in cancers. *Technol Cancer Res Treat*, 21:15330338221134385.
https://doi.org/10.1177/15330338221134385
Rogers S, Macheda ML, Docherty SE, et al., 2002. Identification of a novel glucose transporter-like protein-glut-12. *Am J Physiol Endocrinol Metab*, 282(3):E733-738.
https://doi.org/10.1152/ajpendo.2002.282.3.E733
Salmena L, Poliseno L, Tay Y, et al., 2011. A cerna hypothesis: The rosetta stone of a hidden rna language? *Cell*, 146(3):353-358.
https://doi.org/10.1016/j.cell.2011.07.014
Saxena K, Jolly MK, Balamurugan K, 2020. Hypoxia, partial emt and collective migration: Emerging culprits in metastasis. *Transl Oncol*, 13(11):100845.
https://doi.org/10.1016/j.tranon.2020.100845
Seeber LM, Horree N, Vooijs MA, et al., 2011. The role of hypoxia inducible factor-1alpha in gynecological cancer. *Crit Rev Oncol Hematol*, 78(3):173-184.
https://doi.org/10.1016/j.critrevonc.2010.05.003
Sexton RE, Hallak MNA, Uddin MH, et al., 2020. Gastric cancer heterogeneity and clinical outcomes. *Technol Cancer Res Treat*, 19:1533033820935477.
https://doi.org/10.1177/1533033820935477
Shi Y, Zhang Y, Ran F, et al., 2020. Let-7a-5p inhibits triple-negative breast tumor growth and metastasis through glut12-mediated warburg effect. *Cancer Lett*, 495:53-65.
https://doi.org/10.1016/j.canlet.2020.09.012
Shu J, Xia K, Luo H, et al., 2024. Dars-as1: A vital oncogenic lncrna regulator with potential for cancer prognosis and therapy. *Int J Med Sci*, 21(3):571-582.
https://doi.org/10.7150/ijms.90611
Shu L, Zhang W, Huang C, et al., 2020. Lncrna anril protects h9c2 cells against hypoxia-induced injury through targeting the mir-7-5p/sirt1 axis. *J Cell Physiol*, 235(2):1175-1183.
https://doi.org/10.1002/jcp.29031
Sulaiman R, De P, Aske JC, et al., 2023. Patient-derived primary cancer-associated fibroblasts mediate resistance to anti-angiogenic drug in ovarian cancers. *Biomedicines*, 11(1)
https://doi.org/10.3390/biomedicines11010112
Sun R, Meng X, Pu Y, et al., 2019. Overexpression of hif-1a could partially protect k562 cells from 1,4-benzoquinone induced toxicity by inhibiting ros, apoptosis and enhancing glycolysis. *Toxicol In Vitro*, 55:18-23.
https://doi.org/10.1016/j.tiv.2018.11.005
Tan YT, Lin JF, Li T, et al., 2021. Lncrna-mediated posttranslational modifications and reprogramming of energy metabolism in cancer. *Cancer Commun (Lond)*, 41(2):109-120.
https://doi.org/10.1002/cac2.12108
Taparra K, Tran PT, Zachara NE, 2016. Hijacking the hexosamine biosynthetic pathway to promote emt-mediated neoplastic phenotypes. *Front Oncol*, 6:85.
https://doi.org/10.3389/fonc.2016.00085
Tong J, Xu X, Zhang Z, et al., 2020. Hypoxia-induced long non-coding rna dars-as1 regulates rbm39 stability to promote myeloma malignancy. *Haematologica*, 105(6):1630-1640.
https://doi.org/10.3324/haematol.2019.218289
Vander Heiden MG, Cantley LC, Thompson CB, 2009. Understanding the warburg effect: The metabolic requirements of cell proliferation. *Science*, 324(5930):1029-1033.
https://doi.org/10.1126/science.1160809
White MA, Tsouko E, Lin C, et al., 2018. Glut12 promotes prostate cancer cell growth and is regulated by androgens and camkk2

signaling. *Endocr Relat Cancer*, 25(4):453-469. https://doi.org/10.1530/ERC-17-0051

Wicks EE, Semenza GL, 2022. Hypoxia-inducible factors: Cancer progression and clinical translation. *J Clin Invest*, 132(11) https://doi.org/10.1172/JCI159839

Xing C, Sun SG, Yue ZQ, et al., 2021. Role of lncrna lucat1 in cancer. *Biomed Pharmacother*, 134:111158. https://doi.org/10.1016/j.biopha.2020.111158

Xiong Y, Lei F, 2021. Slc2a12 of slc2 gene family in bird provides functional compensation for the loss of slc2a4 gene in other vertebrates. *Mol Biol Evol*, 38(4):1276-1291. https://doi.org/10.1093/molbev/msaa286

Xu Q, Deng F, Qin Y, et al., 2016. Long non-coding rna regulation of epithelial-mesenchymal transition in cancer metastasis. *Cell Death Dis*, 7(6):e2254. https://doi.org/10.1038/cddis.2016.149

Xu Z, Jin H, Duan X, et al., 2021. Lncrna psma3-as1 promotes cell proliferation, migration, and invasion in ovarian cancer by activating the pi3k/akt pathway via the mir-378a-3p/galnt3 axis. *Environ Toxicol*, 36(12):2562-2577. https://doi.org/10.1002/tox.23370

Yang L, Xie HJ, Li YY, et al., 2022. Molecular mechanisms of platinum-based chemotherapy resistance in ovarian cancer (review). *Oncol Rep*, 47(4) https://doi.org/10.3892/or.2022.8293

Yang S, Ji J, Wang M, et al., 2023. Construction of ovarian cancer prognostic model based on the investigation of ferroptosis-related lncrna. *Biomolecules*, 13(2) https://doi.org/10.3390/biom13020306

Zhang D, Tian X, Wang Y, et al., 2024. Polyphyllin i ameliorates gefitinib resistance and inhibits the vegf/vegfr2/p38 pathway by targeting hif-1a in lung adenocarcinoma. *Phytomedicine*, 129:155690. https://doi.org/10.1016/j.phymed.2024.155690

Zhang K, Kong X, Feng G, et al., 2018. Investigation of hypoxia networks in ovarian cancer via bioinformatics analysis. *J Ovarian Res*, 11(1):16. https://doi.org/10.1186/s13048-018-0388-x

Zhou M, Cheng H, Fu Y, et al., 2021. Long noncoding rna dars-as1 regulates tp53 ubiquitination and affects ovarian cancer progression by modulation mir-194-5p/rbx1 axis. *J Biochem Mol Toxicol*, 35(10):e22865. https://doi.org/10.1002/jbt.22865

Zhou Z, Ma J, 2019. Mir-378 serves as a prognostic biomarker in cholangiocarcinoma and promotes tumor proliferation, migration, and invasion. *Cancer Biomark*, 24(2):173-181. https://doi.org/10.3233/CBM-181980

Zhu J, Han S, 2021. Downregulation of lncrna dars-as1 inhibits the tumorigenesis of cervical cancer via inhibition of igf2bp3. *Onco Targets Ther*, 14:1331-1340. https://doi.org/10.2147/OTT.S274623

Supplementary information

Fig. S1

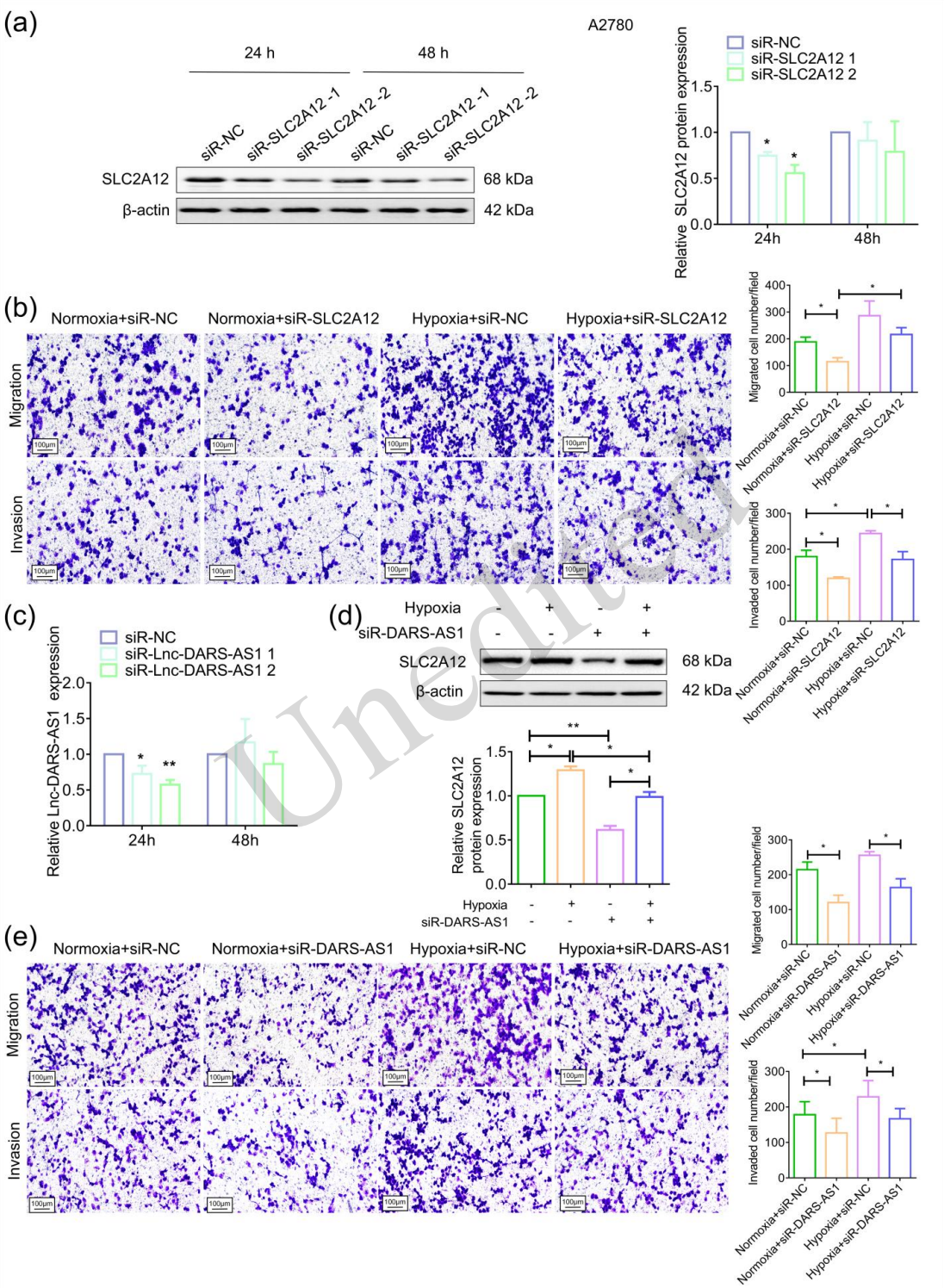

Fig. S1 Lnc-DARS-AS1 promotes the malignant phenotype of A2780 cells through SLC2A12. (S1a) The knockdown efficiency of SLC2A12 was examined by WB assay. (S1b) The migration and invasion abilities of SLC2A12-silenced A2780 cells were examined under normoxic or hypoxic conditions. (S1c) qRT-PCR was used to examine the knockdown efficiency of Lnc-DARS-AS1. (S1d) WB assay was used to detect the expression of SLC2A12. (S1e) The migration and invasion abilities of Lnc-DARS-AS1-silenced A2780 cells were examined under normoxic or hypoxic conditions. All experiments were repeated three times. *p<0.05, **p<0.01.